2nd Turbulence Expert Working Group meeting

ESA ESTEC, Noordwijk, 19-20 February 2008

The operation, maintenance and calibration of turbulent wind sensing systems on research aircraft

Meeting report

Issue 1

Marco Esposito

1 Introduction

The meeting of the EUFAR Expert Working Group on 'Turbulence Measurements' took place in Noordwijk at the Erasmus Centre of ESA ESTEC on the 19th and 20th of February 2008.
Up to 20 experts from Netherland, Germany, Italy, Spain, Switzerland, France and the USA attended the workshop and formed a well mixed group of scientists, users of research infrastructure, operators of research aircraft and developers of new instrumentation. It is well known that the presence of the aircraft in the air is a cause of errors for the measuring instruments; hence the aircraft disturbs the air that it flies through, thereby also disturbing the airdata measurements.
The aim of the meeting was on one hand answer to the questions raised during the first Turbulence EWG meeting held one year before in brauwnsweigh. On the other hand to summarize the best practices that the operators of research aircrafts should do ensuring well calibrated wind/turbulence to deliver to the scientific community. During the first Turbulence Expert Working Group it had been detected that there is still an unsatisfied demand for documentation of turbulence measurements, especially of students and junior scientists visiting the EUFAR website and not knowing about measuring turbulence, and that has to be clarified what constitutes "turbulence measurements". It would be helpful to have a compendium of measurement techniques in use on the EUFAR fleet. This would implicate a detailed description of the used sensors (accuracies, resolutions, time response, limitations…), measurement platforms as well as data processing and calibration techniques. There also should be a list of references/literature available on the EUFAR website. Therefore, with the second Turbulence meeting an attempt to fill these gaps, at least in part, has been made.

During the first session an overview of research platforms, present instrumentation and sensor developments, current/past campaigns, scientific needs and existing problems was given in short presentations by the attendees. These talks provided the basis for the succeeding discussion that resulted in suggestions and ideas for future activities and recommendations to the scientists, aircraft operators and funding agencies.

1.1 Agenda

In the following the agenda of the meeting:

Tuesday 19 Febraury

1. 9:30 – 9:40 Welcome.
   Marco Esposito, CNR ISAFoM,
   Present affiliation: cosine Research BV

2. 9:40 -10:00 ERASMUS Centre activities.
   Massimo Sabbatini, ESA ESTEC

3. 10:00 -10:20 EUFAR activities.
   Marco Esposito, CNR ISAFoM

4. 10:20-10:50 Cosine Research BV, main activities.
   Stefan kraft, cosine Research BV

5. 11:30 - 12:00 Wind calculation from the Skyarrow ERA Aircraft.
   Marco Esposito, CNR ISAFoM

6. 12:00 – 12:30: NLR facilities to measure turbulence in flight
   Wim Bonnee, NLR

7. 12:30 – 13:00 Sensor system of the Polar 5
   Matthias Crèmer, Technische Universität Braunschweig

8. 14:30 – 15:00 Calculation of the wind vector using the M2AV,
   Jens Bange and *Aline van den Kroonenberg, Technische Universitaet Braunschweig*

9. 15:00 – 15:30 High-rate air motion measurements from the NCAR C-130 aircraft: latest improvements and ongoing investigations
   Marie Lothon, UMR-CNRS

10. 15:30 – 16:00 A comparison of two methods for calibrating wind gust-probe systems on aircraft.
    Jeff French, Department of Atmospheric Science, University of Wyoming

11. 16:00 – 16:30 Wind measurement system of the Dornier 128-6
    Mark Bitter, Technische Universität Braunschweig

12. 16:30 – 17:00 Wind basic measurement on INTA aircraft
    Oscar Serrano, INTA

Wednesday 20 Febraury

1. 9:00 – 9:30 Wing and engine effects on turbulence measurements with research aircraft
   John Kalogiros, National Observatory of Athens

2. 9:30 – 10:00 Use and calibration of existing probe @MetAir,
   Bruno Neninger, Metair

3. 10:30 – 11:00 A new modular turbulence probe system project
   Bruno Neninger,Metair

4. Discussion

2. Presentation Session

Part of the two-day meeting was covered by the speeches of the attendees, where they had the opportunity to show their procedures in measuring, calculate and calibrate the wind sensing systems installed onboard different kind of aircrafts, as well as results from past campaigns.

2.1 Abstracts

In the following the presentation abstracts:

2.1.1 Operating the Skyarrow ERA aircraft

Marco Esposito
CNR ISAFoM, Naples, Italy

The three-dimensional wind vector is computed by taking the vector sum of the aircraft relative air velocity and the ground-relative aircraft velocity. The theory of the subsonic potential flow past a sphere is presented as a preamble to the calculation of the attack and sideslip angles, dynamic and static pressure and the true air speed of the aircraft. Those quantities are referred to the aircraft coordinate system, to rotate them in the earth coordinate system the blending in frequency space, by taking the Fourier transform technique to recover the attitude angles at the right frequency, is presented and the results on test data set are shown. The same technique is presented to recover the GPS data velocity from the low acquisition frequency to the right frequency needed to calculate the wind vector.
Dynamic calibration and systems performance tests conducted by evaluating the computed wind vector during certain prescribed flight manoeuvres. Different calibration flights performed during the past years are shown, as well as consideration on the state of the atmospheric boundary layer by means of vertical profile and data results.

2.1.2 High-rate air motion measurements from the NCAR C-130 aircraft: latest improvements and ongoing investigations

By M. Lothon(1), D. H. Lenschow(2), A. Schanot(2) and R. Friesen(2)
(1) Universit´e de Toulouse, Laboratoire d'A´erologie - CNRS UMR 5560, Toulouse, France
(2) National Center for Atmospheric Research, Boulder CO, USA

The use of circular flight tracks during some recent field experiments involving the NCAR C-130 aircraft in the atmospheric boundary layer have brought out some errors in the high rate air motion measurements of the gust probe radome. The circles were flown mainly to estimate the mesoscale divergence, which has a very stringent accuracy requirement. But they also revealed a spurious dependency of the momentum flux vector on the heading angle. Since then, the NCAR Research Aviation Facility has improved the quality of velocity fluctuation measurements with more refined estimates of time lags for different sensor outputs, changes in low-pass filtering, a new static pressure port calibration and a new GPS unit. We will present the discrepancies in the observed velocity spectra and momentum fluxes, and the results obtained with the improved system and new calibration. Some issues remain unresolved. For example, vertical velocity spectra in the inertial subrange are steeper than the predicted -5/3 slope; we strongly suspect a time-dependent upwash contribution to the measured attack angle at high frequencies. We will present our results and ongoing work in this area, and discuss possible correction techniques. Anyone can also have access to the report by Allen Schanot about wind correction in DYCOMS-II dataset, following part of my work: http://www.eol.ucar.edu/raf/Projects/DYCOMS-II/wind_corrections.html

2.1.3 Calculation of the wind vector using the M2AV

Jens Bange and Aline van den Kroonenberg
Technische Universitaet Braunschweig
Institut fuer Luft- und Raumfahrtsysteme

The M2AV is a self constructed model aircraft with two electrically powered engines and a wingspan of two meters. The maximum take-off weight is 4.5 kg (the M2AV is therefore classified as an model plane which simplifies authority issues), including 1.5 kg of payload. It is hand-launched which makes operation of the aircraft easy. With an endurance of approximately 50 minutes, the range accounts for 60 km at a cruising speed of 20 m/s. The M2AV is capable of performing turbulence measurements (wind vector, temperature and humidity) within the troposphere and offers an economic component during meteorological campaigns. The meteorological sensors are mounted on a noseboom to minimise the aircraft's influence on the measurements and to position the sensors closely to each other. Wind is measured via a small five-hole probe, an inertia measurement unit and GPS. The flight mission (waypoints, altitudes, airspeed) is planned and assigned to the aircraft before the semi-automatic launch. The flight is only controlled by the on-board autopilot system which only communicates with a

ground station (laptop PC) for the exchange of measured data and command updates like new waypoints etc. The talk will be focussed on the wind measurements, 5HP calibration and the in-flight wind calibration technique. Turbulence measurements were made during a field campaign in Lindenberg, Germany. M2AV measurements of wind are compared with the 99m-mast and sodar.

2.1.4 Wing and engine effects on turbulence measurements with research aircraft

John Kalogiros
Institute of Environmental Research and Sustainable Development,
National Observatory of Athens, Greece

Flow distortion is a major issue in the measurement of wind turbulence with gust probes mounted on a nose boom, at the radome or under the wing of research aircraft. These effects can be identified with actual data from in flight maneuvers or sampling in the atmospheric boundary layer. Engine effects are more dependent on the specific aircraft, while wing aerodynamic effects are more general. The first effects are due to the slipstream of the engines and may become evident during increase of engine power (like in the time period of maneuvers). An example analysis is shown for propeller aircraft with engines on the wings and a radome pressure probe for turbulence measurements. Wing effects on vertical air velocity are mainly due to the wing upwash. Even though it can be easily detected with calibration flight maneuvers it has a decreasing effect with decreasing size of turbulent eddies. An in-flight method using typical turbulence data is described in order to find the frequency response of the wing to turbulence and correct turbulence time series. Examples of errors introduced to turbulent fluxes by these flow distortions are given.

2.1.5 NLR facilities to measure turbulence in flight

Henk Jentink, Ger Nielen
Flight Test Systems & Applications,
Wim Bonnee
Cockpit and Flight Operations
National Aerospace Laboratory NLR
Anthony Fokkerweg 2
1059 CM Amsterdam

The Netherlands
email jentink@nlr.nl
http://www.nlr.nl

The research aircraft and the instrumentation of NLR to measure turbulence is presented. Different applications are shortly discussed and parameters determining the accuracy are identified.

2.1.6 Turbulence measurements using a small flexible wing weight shift control aircraft: Advantages and additional problems encountered.

Wolfgang Junkerman

A small size weight shift controlled aircraft was equipped with a standard turbulence noseboom probe coupled to a fast inertial navigation system (RT3000, Oxford technologies).
Experience with calibration flights show that the flexible setup of the gondola under the flexible wing has some advantages but the flexibility of the aircraft wing assembly and weight shift control of the aircraft imposes several restrictions to standard processes for in flight calibrations. Current work is in progress including additional parameters describing the configuration and attitude of the flexible aircraft setup

2.1.7 Turbulence and Wake Vortex Measurement with the Dornier 128-6

Mark bitter

The Dornier 128-6 is equipped with a scientific instrumentation which is specialized for meteorological measurements in the lower atmosphere. The standard instrumentation consists of a nose boom which contains sensors for all main meteorological data such as temperature, pressure, humidity and airspeed-vector (wind-vector). Additional wind measurement stations can be installed on each wing tip and the vertical stabilizer. The position and attitude of the aircraft is obtained by an integrated system using the Global Position System (GPS) and an inertial laser navigation platform.

CFD calculations were made and wind tunnel tests were performed to develop the meteorological sensor package placed in the nose boom of the Dornier 128-6. The wind tunnel calibration of the 5-hole probe was validated by an in-flight calibration

which was performed during flight tests over the North Sea in high (FL95) and low altitude (about 100m).

For the alpha / beta calibration, the angle of side slip has been stepwise varied from -10° to 10° at airspeeds gradually increasing from 90 to 150kt to vary the angle of attack. Thus, more than 50 combinations of alpha and beta were flown.

A typical flight maneuver for the dynamic and static pressure calibration is to fly a rectangle with legs of equal duration e.g. 60s (wind method). The heading of these legs were oriented parallel or orthogonal to the mean wind direction. Initially the dynamic and static pressure calibration was performed with the use of a trailing bomb.

Furthermore dynamic maneuvers completed the test pattern.

As an example for the four point wind and turbulence measurement system, a wake vortex encounter flight test is explained. A smoke generator has been installed on the ATTAS to visualize its wake vortex. The Dornier 128-6 performed encounter flights from each side of the vortex. The four wind measurement stations measured the vortex field with a small local resolution. It showed peaks in the vertical wind component of about 15m/s within a distance of 1 to 2m. The results were used in the "s-wake" project for the validation of wake vortex models.

3. Discussion Session

The discussion session took place in the afternoon of the second day of the meeting and focused on the topics raised during the presentation session as explained in the following.

3.1 The different approaches in calibrating wind sensing systems

Different approaches in calibrating the wind sensing system on board research aircrafts were discussed. As shown in the abstracts and in the calibration procedure summaries, kindly delivered by a number of attendees and merged in this document, two main procedures are currently used in the airborne research community. The former is based on the standard "Lenshow maneuvers", it foresees flying in smooth air above the Planetary Boundary Layer (PBL), where homogeneous and free of turbulence wind field is expected to be found. This approach ensures that as many variables as possible are held constant during a single maneuver, and isolating errors source is made easily. The set of maneuvers mainly consists of speed variation, skid, pitch, and reversed heading. The latter approach consists of performing the above maneuvers in a single maneuver, minimizing a specific function related with the Turbulent Kinetic Energy (TKE). In this way the optimum calibration factors are found. Applying this procedure results in saving time and costs, which are particularly high when big-size aircrafts are used, since just two sets of maneuver are performed instead of the six maneuvers with the standard method.

A similar approach is used by another operator, still minimizing a similar function related to the TKE, but the procedure is performed over the whole or part of the measurement flight, instead of using a specific preplanned set of maneuvers. In this case performing "ad hoc" maneuvers is not needed anymore, resulting in a much more efficient mission operation scenario, saving even more time and money than in the second approach described above.

The advantages and disadvantages of those approaches have been discussed. The standard Lenschow maneuvers ensure isolating each single error source in measuring the mean wind vector and the air turbulence, when instead the alternative approach returns the overall performance status and calibration factors of the wind sensing system, without the possibilities to trouble shoot the potential problems present in the system.

The attendees agreed that a comparison of the two methods has to be done, applying both the procedures on the same wind system, analyzing the results. Research groups are already working on it, and results will be shown in a dedicated paper in the near future.

3.2 Wind sensing systems accuracy

The second topic discussed during the meeting was the accuracy evaluation of wind sensing systems. Even though several operators currently define their own system accuracy, it is well known that it is hard to decide a `number` to assess the accuracy. Actually, the wind measurement has different accuracies in respect to different operating conditions. Those are mainly related with the aircraft dynamics during the measurement mission. Moreover, the performance of the wind sensing system changes with the frequency. The first suggestion was to put flags in the data file that the operators deliver to the scientific users, with which the best and worst accuracy are reported for different parts of the flight. The same operation can be done in respect to the different frequencies of the data, so the users are able to find out the best compromise in between frequency and accuracy of the turbulence measurement.
Another point is that different processing methods used to calculate the turbulence from the row data could have different results in terms of accuracy; transparent data sets could help in find out the error related to the applied procedure, i.e., the proposal to exchange raw data sets that could be processed by another group with their own software, and to subsequently compare the derived quantities. Such a procedure would most certainly give new insight into the effect of the processing methods.
During the discussion a field campaign with flying-bys above a tower in the North-Sea with several aircraft was proposed.

3.3 Lagrangian and Eulerian references

Shortly was discussed the use of " the lagrangian -6/3 law instead of the Eulerian -5/3 law", and a reference document was delivered (Corrsin (1963)).
It's clear that a measurement by a fast aircraft is quasi Eulerian, but, is suggested to do not take a very strict -5/3 as an ultimate truth. The users should reach a level of reliability of their measurements by other means, in order to be able to TEST the theory under different flow conditions. Not vice versa to adapt the measurements to a limited theory. Let us assume a slow flying aircraft once on the headwind track and once on the tailwind track.

Corrsin's transformation then tells us that there might be a difference between the two spectra! The experience of Metair using the balloons was so to say the slowest possible aircraft. The message is that the users should definitely re-consider such differences when they are using slow microlights, helicopters and Zeppelins.

3.4 Meeting outcome

Hereafter the comments from Hans Richner:

Development of instrumentation and techniques

It is surprising that hardly any new developments took place during the last twenty years. The only exception is GPS: the numerous problems related to position and attitude angles derived from inertial systems have definitely been overcome by using GPS.

What about optical and acoustic systems? Is their use really limited to surface applications? Any initiative to improve existing and/or new sensors, systems, or evaluation procedures should be supported. In that sense it is to be hoped that the Joint Research Activities within EUFAR FP7 can be realized.

Deficiencies

The effects of upwash, vibration, propellers, distorted flow etc. on wind data are obviously still not under control. Also, the different methods for dealing with them might be ok under the conditions assumed. But what about them in situations where the density and/or the flow angles are different? Why is it not possible to place the probe in a position where it is less disturbed by unwanted processes?

In a side discussion I heard that 5-hole-probes are calibrated in wind tunnels using an angular reference frame, which is different from that used for the aircraft. Is this really the case? If yes, is the necessary transformation included in data evaluation?

In those cases where certain parameters are derived from different systems (e.g. ground speed, once from radar and once from in-situ aircraft data), the causes for discrepancies should be seriously investigated.

Calibration and verification

The debate about maneuvers and techniques based on minimizing TKE took place during the meeting. If financially (flight time!) justifiable, both methods should be used; in any case, an attempt should be made to compare the results of the two approaches in case studies.

About future activities:

(i) Although not cheap, direct intercomparisons in form of parallel flights (combined with a data exchange, see below) seem a very good idea. It should be performed under homogeneous atmospheric conditions and over flat terrain. The

idea to realize such an experiment over the North Sea near a meteorological tower seems ideal!

(ii) The attendees support the idea of transparent data sets, i.e., the proposal to exchange raw data sets that could be processed by another group with their own software, and to subsequently compare the derived quantities. Such a procedure would most certainly give new insight into the effect of the processing methods.

Hereafter the comments from ANTEE boundary-layer group in the Laboratoire d'Aérologie of Toulouse:

- A comparison between tower-measured and aircraft-measured turbulence is justified only in the first validation step of a new research aircraft, because one cannot expect better comparison of turbulent fluxes than 20% (see LES studies by Kanda et al or Huang et al about this issue) and it only helps to check that the measurements are realistic.
- We think that for an accurate measurement of the wind, the in-flight maneuvers are the best ways today to adjust the calibration.
- Aircraft to aircraft intercomparison (after solid validation and calibration of each airplane separately) can always be interesting, because if it is done properly, the same air-mass can be probed with the two (or more ?) aircraft.

* For the purpose of estimating the accuracy of both airplanes measurements of the mean wind, it can be done in still air. It is important to check that the airplanes will be able to fly at exactly the same height.

* For the purpose of evaluating the error made on measuring fluxes and other turbulent moments, the aircraft can fly over an homogeneous continental and convective PBL. The difference between the two aircraft should be quite informative, as soon as they fly rigorously the same way, probe the same airmass, at the same height and time.... There will definitely be a difference of sampling in case of different airspeed that we will not be able to avoid, but could try to optimize at least, in the way the legs are flown.

4. Recommendations

From this workshop the following recommendations are given in short form:

4.1 Instrumentation development

During the workshop was noted that not any new developments took place during the last twenty years. Therefore it is strongly recommended to enforce development of a replacement the current technologies to measure wind and turbulence. Sharing the cost of development within EUFAR would be of great benefit for the whole community.

4.2 Recommendations to the Operators

Improved documentation is recommended including the following items:
Sensor package description, description of data processing and error calculation.
Direct intercomparisons in form of parallel flights is suggested. It should be performed under homogeneous atmospheric conditions and over flat terrain. The idea to realize such an experiment over the North Sea near a meteorological tower seems ideal.
Exchange raw data sets that could be processed by another group with their own software, and to subsequently compare the derived quantities. Such a procedure would most certainly give new insight into the effect of the processing methods

4.3 Recommendations to the Funding Agencies

Funding for in-flight intercomparisons is necessary to improve quality of data within EUFAR, and the same to support networking activities in terms of data processing (exchange of raw data-set).

4.4 Recommendations to the Users

Information exchange between operator and user is an iterative process. It is therefore highly recommended for users to contact the operator in early stage of their project.

5. Operators In flight calibration procedures

In this section procedure that operators are using in calibrating their wind sensing system are presented in detail.

5.1 Calculation of the wind vector using the SkyArrow aircraft

Marco Esposito, CNR ISAFoM, Naples, Italy

5.1.1 Three-dimensional wind vector

The three-dimensional wind vector is computed by taking the vector sum of the aircraft relative air velocity and the ground-relative aircraft velocity.

$$\overline{V} = \overline{V_p} + \left[\overline{\overline{M}}\right] \times \overline{V_a'} \qquad (5.1)$$

Figure 5.1 shows the block diagram for the airborne wind calculation chain.

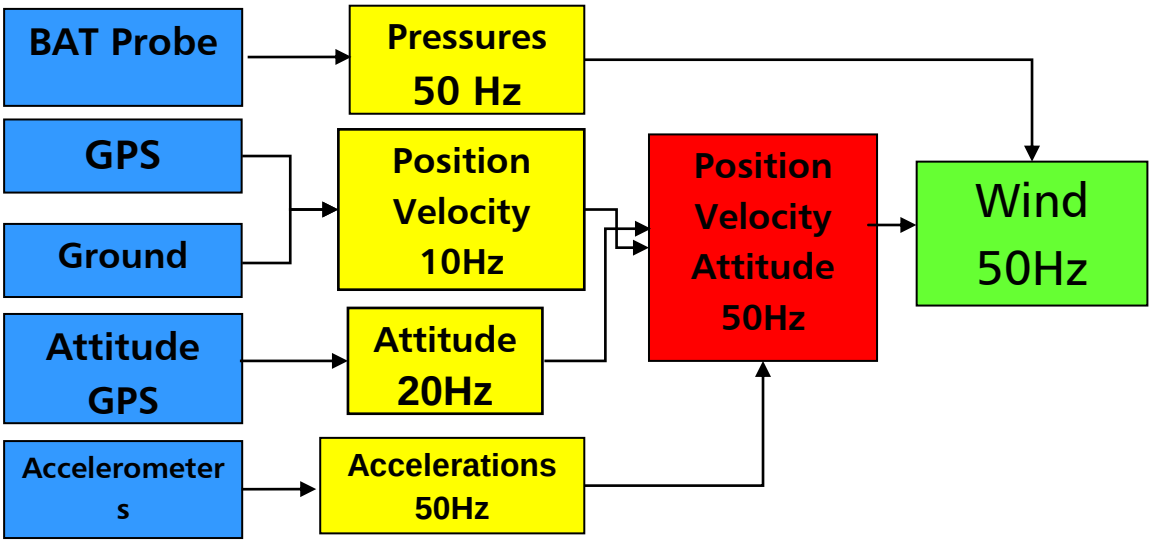

Figure 1: wind calculation block diagram

The diagram shows the sensors used (blue boxes), the data collected and the acquisition frequency (yellow boxes), and how those data are merged to obtain

congruent frequencies (red box), to obtain the three dimensional wind vector in the earth centred inertial reference frame (green box).
These data are used to calculate the motion of the sphere in respect to the ground and to calculate the matrix to rotate the data from the aircraft reference to the earth reference. To calculate the motion of the sphere in respect the air we use the pressure measurements provided by the sphere itself, and then, making the sum we calculate the three dimensional wind vector.
To better explain the algorithm, we use to divide the procedure in the following steps:

1. Flow angles calculation
2. True air speed calculation
3. Development of rotation matrix $\overline{\overline{M}}$ to rotate vectors from "*Body Reference Frame*" to "*Inertial Reference Frame*".
4: Ground speed calculation

Flow angles

In High number of Reynolds number flow past a sphere, the pressure distribution for potential flow is:

$$P_\gamma - P_s = \frac{1}{2}\rho U^2\left(1-\frac{9}{4}\sin^2\gamma\right) \qquad (5.2)$$

where $q = \frac{1}{2}\rho U^2$ is the dynamic pressure, p_s is the static pressure, and p_γ is the pressure at an angle γ from the flow stagnation point on the sphere.

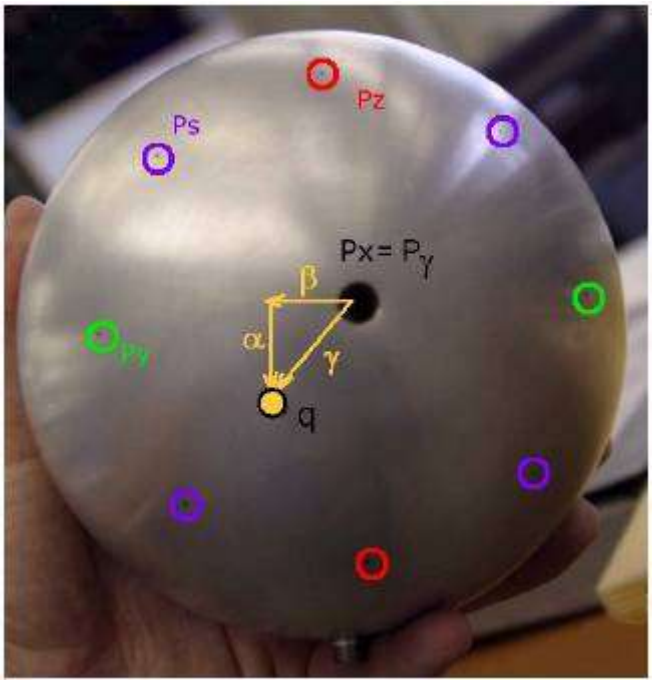

Figure 2: ***The pressure sphere: highlighted the nine holes for static, total and differential pressure measurements***

At any given time, the relative wind vector will form an angle with the probe *x* axis, as shown in Figure 3. The relative wind can have both an angle of attack *α* in the *x-z* plane (similar to latitude on the earth) and angle of sideslip *β* in the *x-y* plane (similar to longitude). Nonzero values of these angles will directly lead to displacements of the flow stagnation point away from the central port.

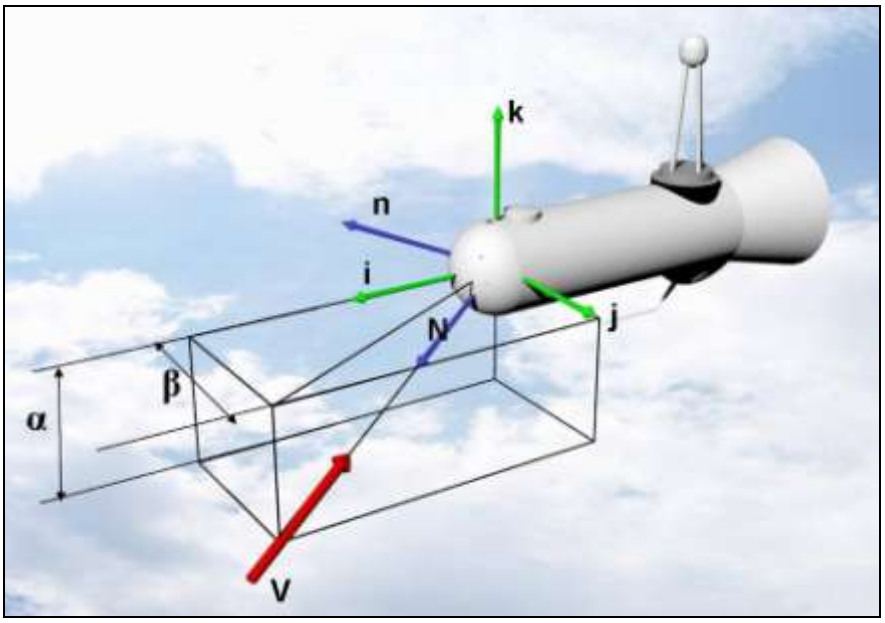

Figure 3*: flow angles in the sensor reference*

After mathematical manipulation we get the following equations representing the angles of attach and sideslip, and dynamic pressure:

$$H_\alpha = \frac{2}{9}\frac{\delta\hat{P}_z}{\delta\hat{P}_x} \tag{5.10}$$

$$H_\beta = \frac{2}{9}\frac{\delta\hat{P}_y}{\delta\hat{P}_x} \tag{5.11}$$

The flow angles can be obtained as:

$$\tan\alpha = 4H_\alpha\left[1+\sqrt{1+8\left(H_\alpha^2+H_\beta^2\right)}\right]^{-1} \tag{5.12}$$

$$\tan\beta = 4H_\beta\left[1+\sqrt{1+8\left(H_\alpha^2+H_\beta^2\right)}\right]^{-1} \tag{5.13}$$

And the dynamic pressure as:

$$q = \frac{8}{9}\frac{\delta p_x}{\sin^2\phi_r}\frac{1+\tan^2\alpha+\tan^2\beta}{1-\tan^2\alpha-\tan^2\beta} \tag{5.14}$$

True air speed

When combined with a temperature measurement *T*, the computed values of *α*, *β*, and *q* provide the information required to estimate the True Air Speed V_a. The temperature must first be corrected for adiabatic heating resulting from the aircraft motion. The corrected temperature *T'* is related to the measured temperature *T* through the equation (Lenschow 1986; Leise and Masters 1991):

$$T' = T\left(1 + r\frac{\gamma - 1}{\gamma}\frac{q}{p_s}\right)^{-1} \quad (5.17)$$

Once the Mach number and the corrected temperature are known the true air speed can be computed as (Lenschow 1986):

$$U_a = M\sqrt{\gamma R_m T'} \quad (5.18)$$

The three components of the relative-wind vector are then obtained from the equations:

$$\hat{u}_a = -\frac{U_a}{\sqrt{1 + \tan^2\alpha + \tan^2\beta}} \quad (5.19)$$

$$\hat{v}_a = -\hat{u}_a \tan\beta \quad (5.20)$$

$$\hat{w}_a = -\hat{u}_a \tan\alpha \quad (5.21)$$

The aircraft-relative air velocity is determined by the gust probe system and is rotated into the earth coordinate system using a transformation matrix, $\overline{\overline{M}}$ defined by the aircraft attitude as is showed in the next section.

The rotation matrix

Some of the aircraft sensors, such as the GPS subsystem, provide vector quantities that are oriented in the earth coordinate system (x; y; z). Others, such as the probe sensors, produce vectors in the probe coordinates (x'; y';z'). The relationship between these coordinate systems varies with time and must be measured so that the proper rotations can be applied to vector quantities. Three angles are used to express the relative orientation of the two systems: the roll ϕ, pitch θ, and yaw ψ .
The Sky Arrow has two sets of three-dimensional accelerometers mounted both on the nose and in the Aux Box, close to the centre of gravity of the aircraft. The difference between the two measurements gives information about the attitude of the aircraft.
The acceleration data are collected at the frequency of 50Hz, and then they can be used to resample the attitude data from 20Hz to 50Hz, so they will be comparable with the pressures and gases data collected by the others sensors mounted on the airplane.
Equation 5.22 shows that the difference between the z-axes acceleration measured on the nose, and the z-axes acceleration measured on the centre of gravity divided by the distance between the two sets, is equal to angular acceleration around the y-axes, that is the second derivative of the pitch angle.

$$\frac{\partial \theta^2}{\partial t^2} = \frac{\hat{a}_z - \hat{a}_{bz}}{d} \qquad (5.22)$$

The same information is recovered for the yaw angle by means of the y-axis accelerations (equation 5.23).

$$\frac{\partial \psi^2}{\partial t^2} = -\frac{\hat{a}_y - \hat{a}_{by}}{d} \qquad (5.23)$$

These signals are blended in frequency space by taking the Fourier transform of all the time series. Using the Fourier transform $\Theta(f)$ of the pitch θ at frequency *f* as an example, the blending took the form:

$$\Theta(f) = (1-\eta)\Theta_l(f) + \eta\Theta_h(f) \qquad (5.24)$$

Where $\eta = \eta(f)$ is a weighting function between 0 and 1. Below a specified frequency *f*1, η was set equal to zero. Above another frequency *f*2 (> *f*1) , η was unity. At frequencies *f* between *f*1 and *f*2, the weighting function took the form:

$$\eta = \frac{\log(f/f_1)}{\log(f_2/f_1)} \tag{5.25}$$

The use of Fourier transforms in blending the GPS and accelerometer data had another benefit in dealing with the accelerometer data. As shown in Eqs.(5.22) and (5.23), the accelerometers provide the second derivatives of the pitch and yaw angles.
Thus, the integrations in Eqs.(5.22) and (5.23) were performed by first taking the Fourier transform of the right sides, and then multiplying the resulting Fourier coefficients by the filter function.

$$I(f) = \frac{1}{(2\pi f)^2} \tag{5.26}$$

After the filtering and blending described above were completed, the resulting Fourier transforms were inverse transformed to their corresponding angles ϕ, ϑ, and ψ.
These 50Hz blended angles are the ones that are used to rotate vectors from the probe coordinate system to earth coordinates.
To make the quality of a signal visible relative to the frequencies, a power spectrum is used. It gives a plot of the portion of the signal's power in respect to given frequencies. A power spectrum is the Fourier Transformation of the auto covariance function.
The figures 5.5 and 5.6 show the spectrum of the javad angle signal and of the accelerometer data, and of the blended results. In the last part of the spectrum of the accelerometers is present a strong noise, due probably, since the high sensitivity of the accelerometer sensors, at aliasing effect.
Aliasing means that the frequencies that are above the Nyquist frequency appear the same amount that they exceed the Nyquist Frequency, below the Nyquist Frequency in the power spectrum. In the case of the accelerometers the noise source is probably the vibration present inside the aircraft due for the presence of the engine and the blades.

In fact (Porsen, 2005), with a maximum power at 5800 rpm and so an estimated cruising rpm of 5000 and a 2.27:1 reduction gear ratio, the propeller would rotate with about 2000 rpm during most of the flight time. That is a frequency of 33 Hz.. So for a sampling rate of 50 Hz and accordingly a fny of 25 Hz, this vibration would appear 17 Hz in the power spectra.
To verify the data is used the -5/3 decalaw, also colled the kolmogorv spectrum (Bhattacharjee, 1994).

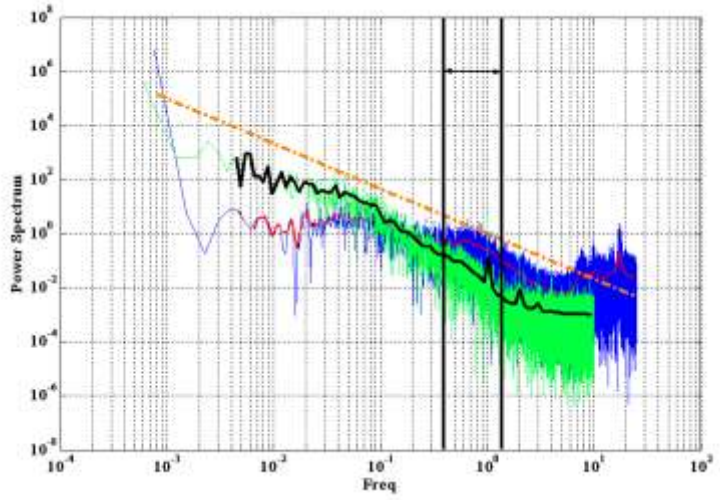

Figure 4*: The spectrum and the mean spectrum, of the javad signal (green) and of the accelerometer data (blue). Highlighted with the black line the interval [f_1 f_2] where is applied the function η, and in orange the .5/3 decay law.*

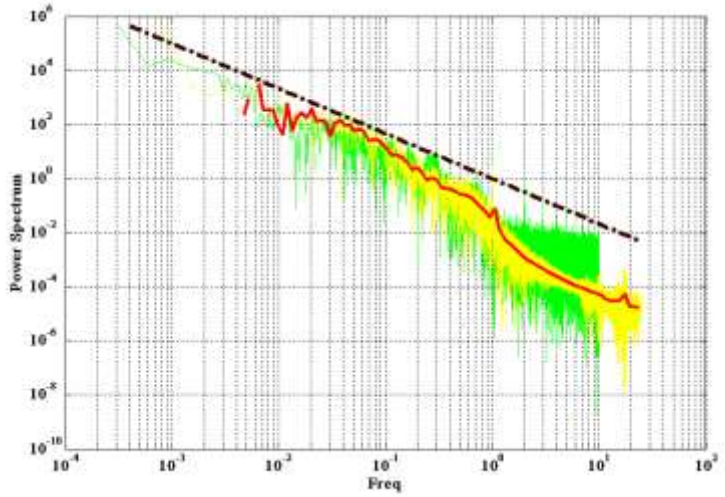

Figure 5*:The spectrum of the blended signal (yellow line), overlapped at the source signals*

Figure 6 shows the time series of the pitch angle both before and after the frequency blending operation. It is visible from both the figures 5.6 and 5.7 that the noise is drastically diminished, in fact the power spectrum of the blended signal do not present the increase of noise at high frequency that before the javad spectrum shows. The spectrum are also compare with the -5/3 decay law. Moreover from Figure 6 is clear that the blended signal is not affected from the random noise that is visible in the source signal in red.

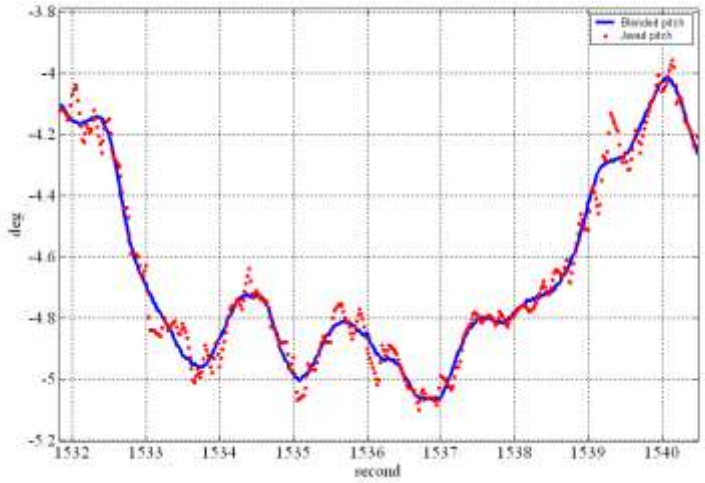

Figure 6: ***The pitch angle time series both before and after the frequency blending. The noise of the javad attitude sensor is filter-out.***

At this point is possible to construct the rotation matrix $\overline{\overline{M}}$, as the following relation:

$$\overline{\overline{M}} = \overline{\overline{M_h}} * \left(\overline{\overline{M_p}} * \overline{\overline{M_r}} \right) \tag{5.27}$$

Where:

$$\overline{\overline{M_r}} = \begin{bmatrix} 1 & 0 & 0 \\ 0 & \cos(\phi) & \sin(\phi) \\ 0 & -\sin(\phi) & \cos(\phi) \end{bmatrix} \tag{5.27}$$

$$\overline{\overline{M_p}} = \begin{bmatrix} \cos(\vartheta) & 0 & -\sin(\vartheta) \\ 0 & 1 & 0 \\ \sin(\phi) & 0 & \cos(\phi) \end{bmatrix} \tag{5.27}$$

$$\overline{\overline{M_h}} = \begin{bmatrix} \sin(\psi) & -\cos(\psi) & 0 \\ \cos(\psi) & \sin(\psi) & 0 \\ 0 & 0 & 1 \end{bmatrix} \tag{5.27}$$

Ground speed

The GPS velocities have the same problem as the attitude angles described in the foregoing section, namely that they did not have a fast enough sampling rate to provide Vp measurements up to the desired 50 Hz.
The same formalism used above is applied for the ground speed.

5.1.2 Wind sensing in-flight calibration

During this maneuver the direction could be straight, at constant cardinal heading (0°, 90°, 180°, or 270° true), wings level, constant airspeed of 70 KIAS, at constant pressure altitude. Altitude variance during this maneuver should be ±10 feet, airspeed variance should be ±1 knot, and heading variance should be ±1° during the entire maneuver.

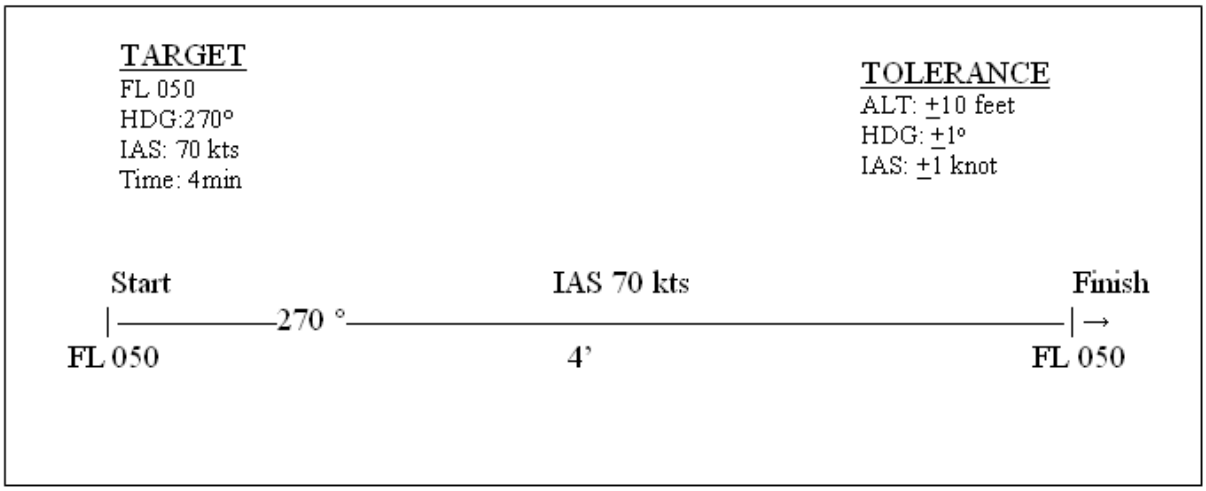

Fig 6.4: The straight and level maneuver plan

From this maneuver is possible to evaluate the influence of the pitch on the average of the computed vertical velocity.

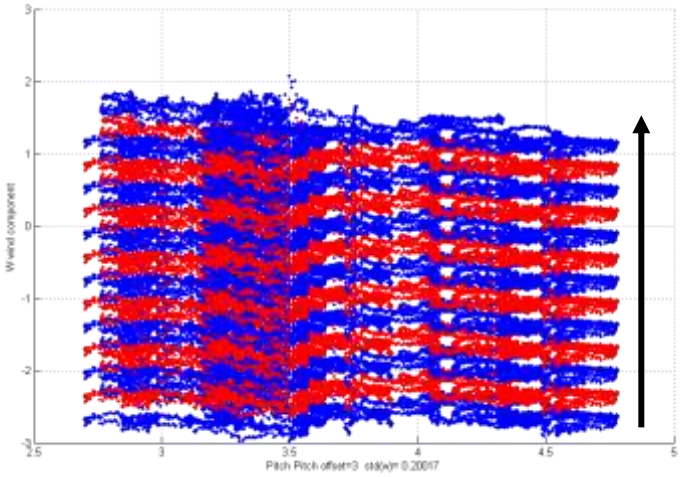

Fig 6.5: The computed vertical wind velocity Vs the pitch angle during the straight and level maneuver

The best pitch offset value is found forcing to zero the mean vertical wind velocity.
In figure 6.5 is shows the computed vertical velocity versus the pitch angle during the straight and level maneuver, at different pitch offset. Running the algorithm for the wind calculation with pitch offset from -3 to 3, is clear that the value for that the mean vertical wind is closest to zero is for pitch offset equal to one.
The result is showed in figure 6.6, where are plotted the mean value of the calculated vertical velocity versus the pitch offset.

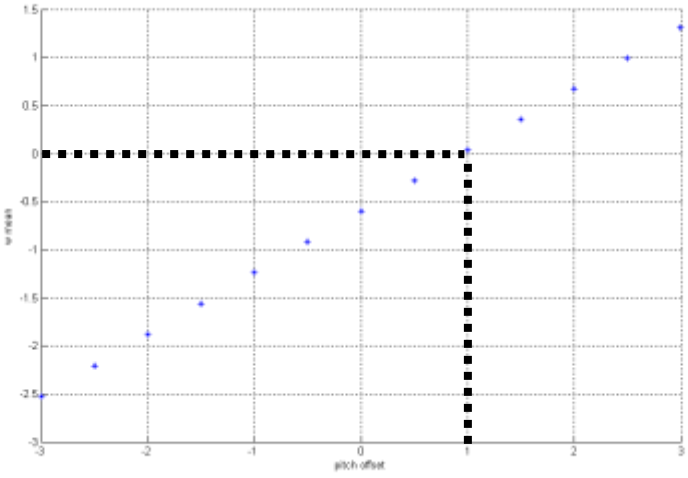

Fig 6.6: the mean of the computed vertical velocity Vs the pitch offset during the straight and level maneuver

Wind Box

This maneuver should begin with the aircraft on a heading of 0° true (due North). The airspeed should be 70 KIAS and the aircraft trimmed for hands-off flight at constant altitude. The transect should be flew at constant airspeed and constant heading for 2 minutes, performing a standard rate turn to the left, maintaining altitude and airspeed during the turn. Aircraft should be rolled out of the turn on the heading 270°, rolling out of the turn on a heading of 180° true (due South). Rolling out on a heading of 90° true (due East), rolling out on heading of 0° true (due North). Altitude variance during this maneuver should be ±10 feet, airspeed variance should be ±1 knot, and heading variance (during the straight portions, of course) should be ±1° during the entire maneuver.

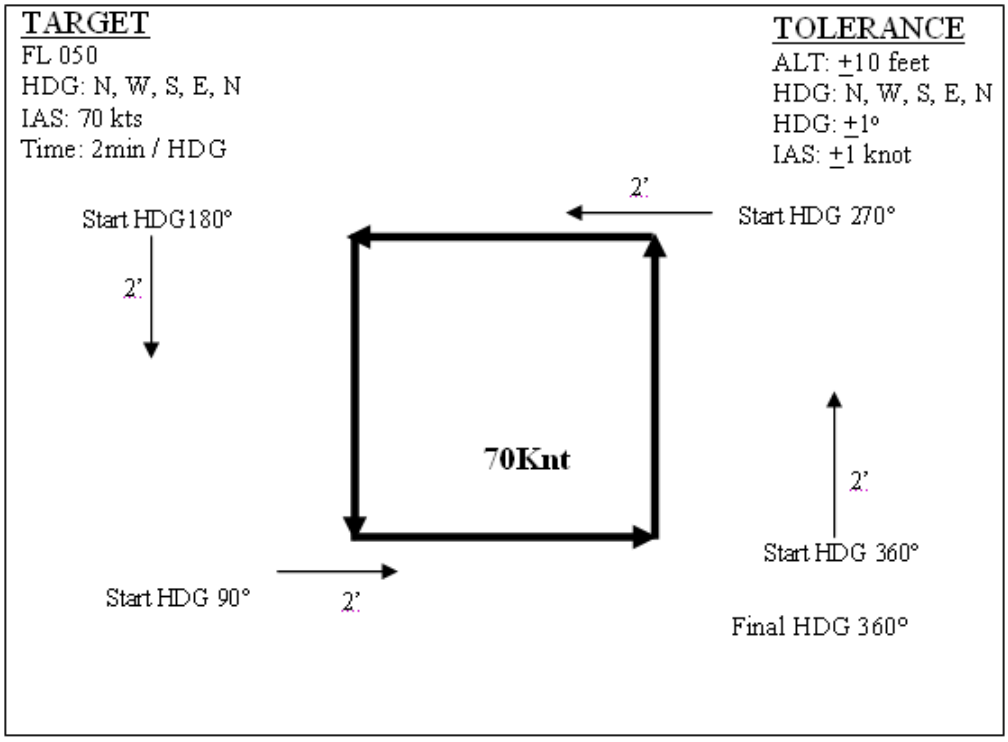

Fig 6.7: The wind box maneuver plan

From the box maneuver is possible to evaluate the best calibration factor for direction and magnitude of the calculated horizontal wind.
Mainly the horizontal wind is influenced by the error in the dynamic pressure computation regards the magnitude, and by the heading offset for the direction.
Flying with an heading of 90°, and after that flying with an heading of 270°, can be evaluated the error on the calculated north wind component, that is the component orthogonal at the flight headings. In fact if the wind field is

homogenous, the value of this component should be the same in both the flight direction.

Figure 6.9 shows the north wind component along the two transect (red=90°, blue=270°) at different heading offset. The best value is of -2.8, that is the point where the two lines have an intersection.

For the influence of the heading offset on the east wind component calculation, from the same consideration above, we have to consider the flight heading toward north and toward south. Figure 6.10 shows the best value at -3.2. Averaging the result above, the best heading offset to minimize the error in the calculation of the horizontal wind is -3.

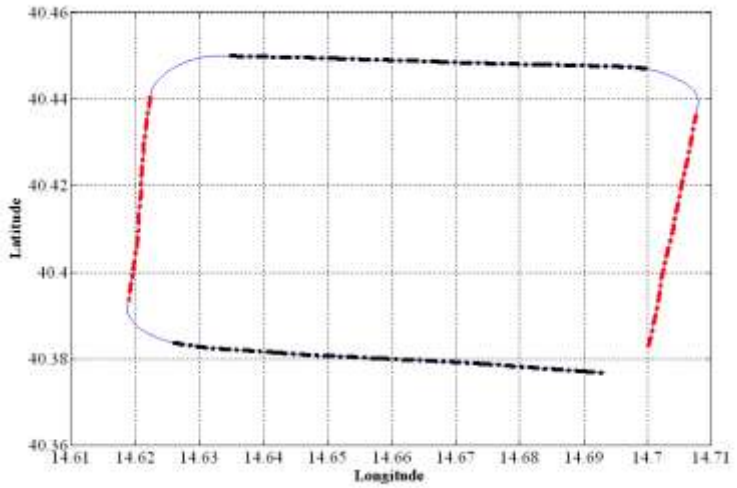

Fig 6.8: The wind box performed during the Calibration flight held on 1th of july 2004

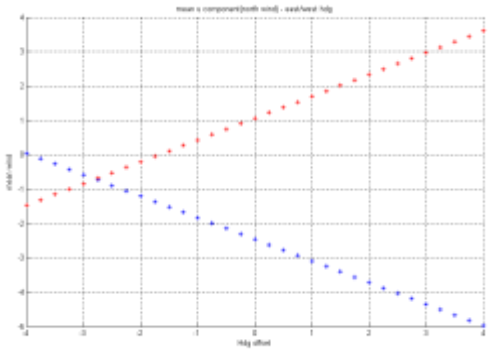

Fig 6.9: variation of the north wind component on the east-west transect, with heading of 90° (red) and heading of 270° (blue) Vs different heading offset

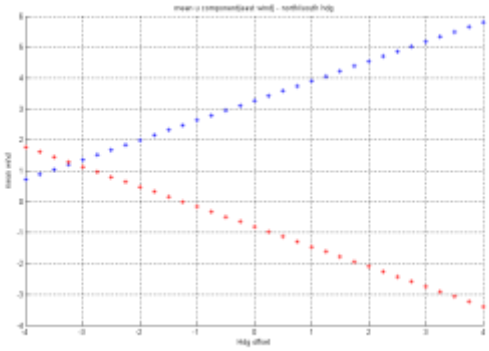

Fig 6.10: variation of the east wind component on the north-south transect, with heading of 0° (red) and heading of 180° (blue) Vs different heading offset

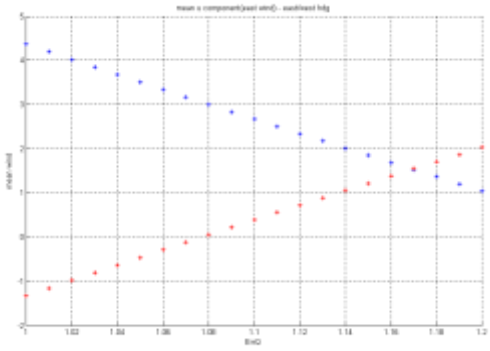

Fig 6.11: variation of the north wind component on the north-south transect, with heading of 0° (red) and heading of 180° (blue) Vs different dynamic pressure offset

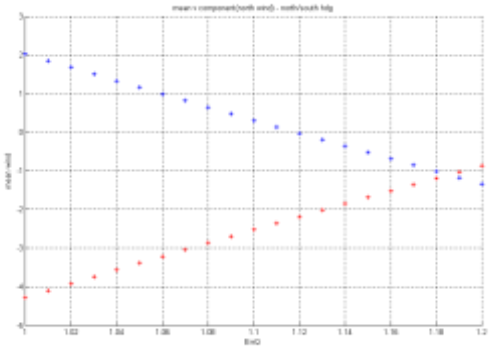

Fig 6.12: variation of the east wind component on the east-west transect, with heading of 90° (red) and heading of 270° (blue) Vs different dynamic pressure offset

The dynamic pressure is different if the aircraft is flying in-wind or out-wind, or in other words if the aircraft had the wind on the nose or on the tail. To minimize the error in the magnitude of the horizontal wind due the variation in dynamic pressure, we must evaluate the north wind component on north-south transect, and east wind component on east-west transect.

Figure 6.11 and 6.12 shows the variation of the north wind component at different dynamic pressure coefficient (ErrQ). The best ErrQ from both the transects is of 1.176.

Acceleration/Deceleration maneuver

This maneuver should be flown at constant pressure altitude, on a constant cardinal heading, wings level. Maintaining a constant airspeed of 110 KIAS, at constant altitude, with the airplane in steady flight. A this time begin a smooth power reduction that allows airspeed to decrease constantly at a rate of 10 knots/minute. The pressure altitude during this maneuver should be constant. Continuing the smooth airspeed reduction until 60 KIAS is attained. This should take 5 minutes to complete. The pitch angle of the aircraft will smoothly increase during this maneuver. Once 60 KIAS is attained begin a smooth power increase that allows airspeed to increase smoothly at a rate of 10 knots/minute. Again, maintain constant pressure altitude and continue the smooth airspeed increase until 110 KIAS is attained. Altitude variance during this maneuver should be ±10 feet, airspeed variance should be ±1 knot, and heading variance should be ±1° during the entire maneuver.

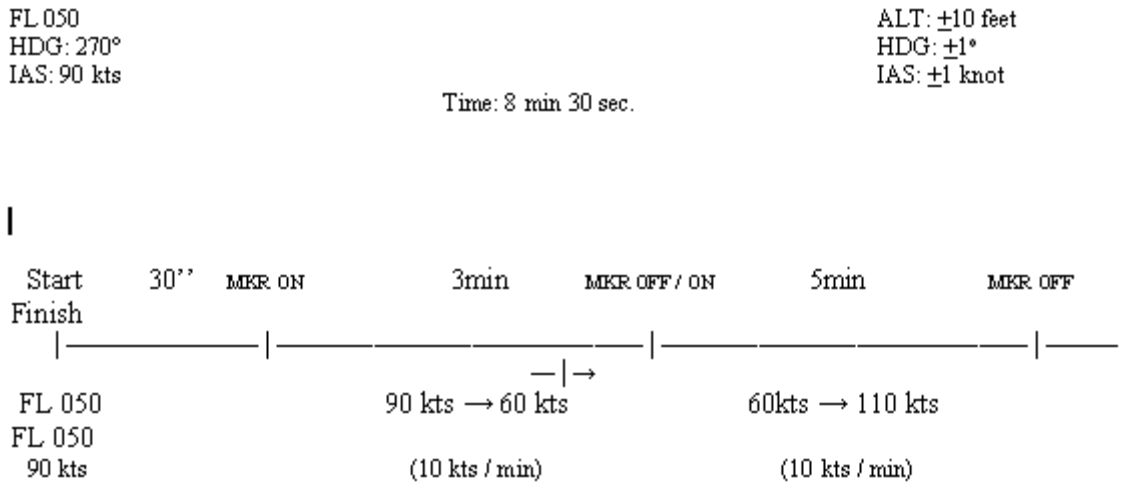

Fig 6.13: the pitch calibration maneuver plan

The wing in generating lift induces, among other things, an upward flow deflection ahead of the airplane (upwash), this directly influence the calculated vertical wind component (Crawford et al,1993).

The upwash effect increases with the lift and then with true air speed of the aircraft. In figure 6.14 is showed the calculated true air speed during the acceleration/deceleration maneuver.

In this maneuver we can see a variation of the airspeed of about 10 m s^{-1}, which is consistent range to evaluate the best calibration factor to minimize the error in the calculated vertical wind component.

Figure 6.15 shows the standard deviation of the vertical wind at different upwash coefficient. The best coefficient is in correspondence of the minimum of the curve, that is the minim variation of the calculated vertical wind component at different upwash effect on the nose of the airplane.
With Kupwash of 0.15 we have a W standard deviation of 0.055 m s^{-1}.

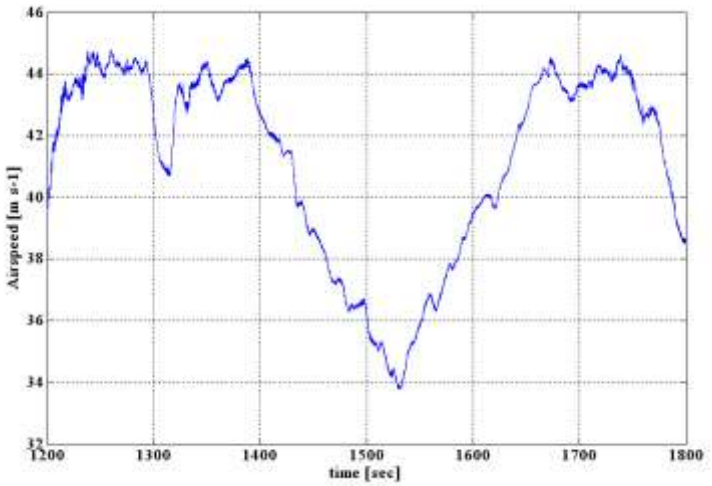

Fig 6.14: time series of the calculated true air speed during the airspeed calibration maneuver

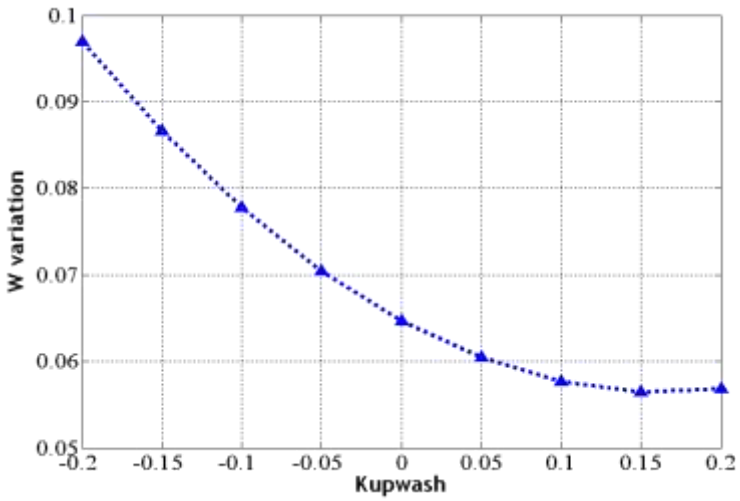

Fig 6.15: variation of standard deviation of the calculated vertical wind component Vs different upwash coefficients

The airspeed maneuver modulates also the attack angle and the pitch angle; since the pitch angle is measured accurately, the error in attack angle can be determined

by comparing the attack angle with the vertical wind component with respect to the earth.

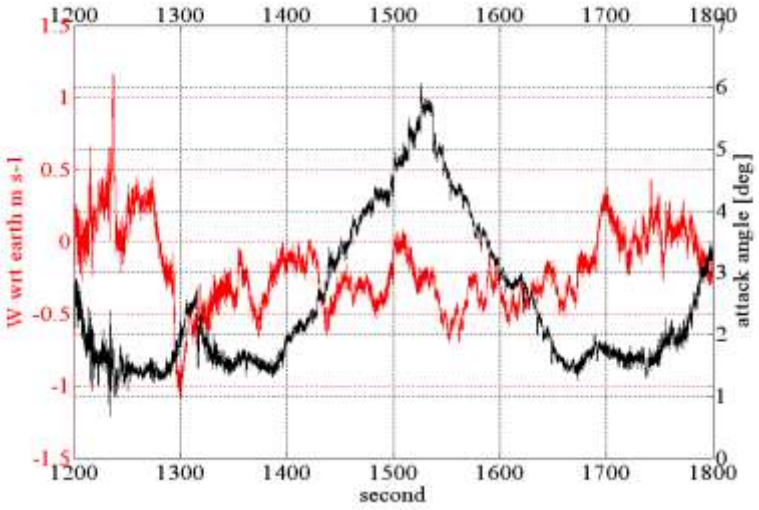

Fig 6.16:the attack angle (black line) compared with the calculated vertical wind velocity (red line) during the acc/dec maneuver

It is possible to see that there isn't a strong correlation between the signals, in fact during the deceleration the pilot forces the aircraft to maintain the altitude, doing this the attack angle increases, and this could results in an error in calculating the vertical wind velocity.

Pitch Up/Down

This maneuver should be flown at constant pressure altitude, flying the airplane at a constant cardinal heading, maintaining 70 KIAS. The first step consist to fly straight and wings level for 30 seconds. Next, the pilot has begin to pitch the airplane up allowing the nose to reach a maximum pitch angle (approximately 5° nose up) in a period of approximately 5 seconds. Immediately after the nose reaches the maximum nose-up angle, begins to pitch the nose down. After 5 seconds, the plane should be nose-level, and the pitch maneuver should continue smoothly until the nose is approximately 5o down. The nose should then be smoothly brought back to level, again taking approximately 5 seconds. The idea is to complete one pitch up/down cycle in 20 seconds. The 20-second cycle should then be smoothly repeated 6 times, taking two minutes for the full maneuver. After completion of the maneuver, the nose should be level and the airplane held straight and level for another 30 seconds. Altitude variance during this slow pitch maneuver should be allowed to vary as necessary, but altitude should always return to the original starting altitude as the plane passes through nose-level. The airspeed variance should be +1 knot and heading variance should be +1° during the entire maneuver.

This procedure should be repeated as outlined above, using a 2.5-second period instead of a 5-second period. This is the medium frequency pitch up/down maneuver. The final pitch up/down maneuver is made at high frequency. The complete pitch cycle (nose up, nose down, nose up) should take approximately 1 second to complete.

Note that this maneuver has the potential to introduce large vertical accelerations on the aircraft unless the pitch angle is carefully monitored.

See figure 6.17 where is showed the procedure explained above.

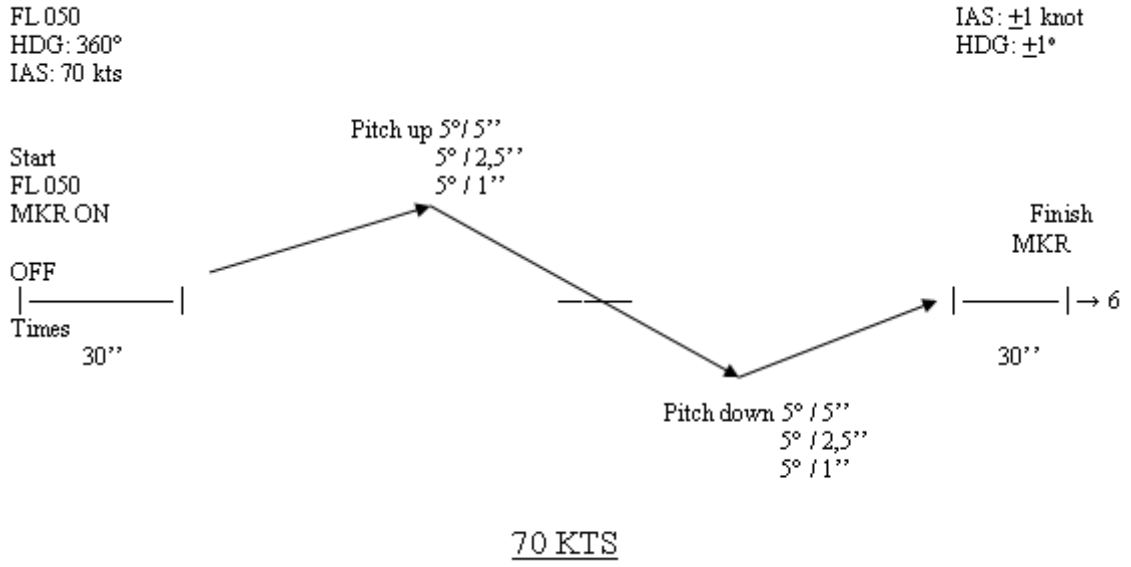

Fig 6.17: pich up/down maneuver procedure

The angle of attack, the pitch angle, the static and dynamic pressures, and the vertical acceleration are synchronized by this manuever. The calibration factors for the measured angle of attack and for the attack angle effect on static and dynamic pressures can be determined very precisely.

For this calibration flight the pilot was not able to apply the entire procedure, as is showed in figure 5.17, the pilot performed an oscillation of a period of 5 seconds (0.2 hz), and 4 oscillation with a period of 2,5 seconds (0.4 Hz).

The "*pitch up/dn*" manuever is used calculate the optimum "*Kalpha*" coefficient, forcing the variance of the calculated vertical wind . The general rule of thumb criterion for acceptable calibration of the system is that peak-to-peak variation in the vertical wind should be less than 10% the variation of the ground-relative aircraft velocity. The high sampling frequency of the air data and of the computed aircraft vertical velocity (50 Hz) is a great benefit for the analysis.

From figure 6.19 is possible to see that the optimum *Kalpha* calibration factor is of 0.205, for what we have a standard deviation for the vertical wind of 0.09 m s^{-1}.

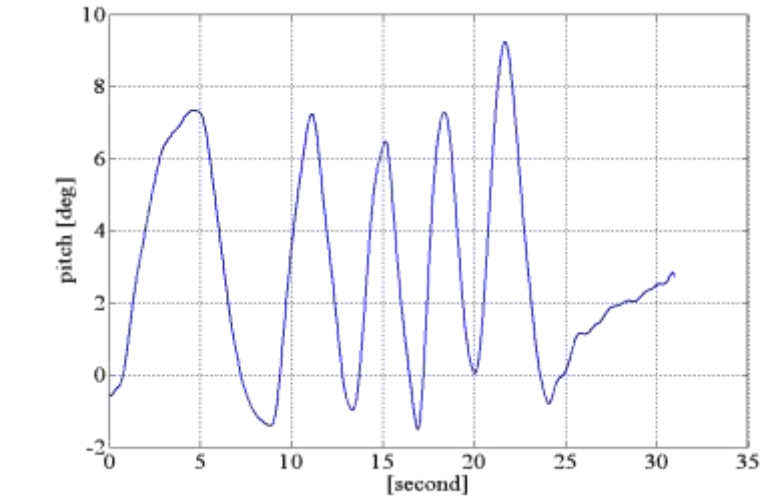

Fig 6.17: the pitch up/down maneuver performed during the calibration flight

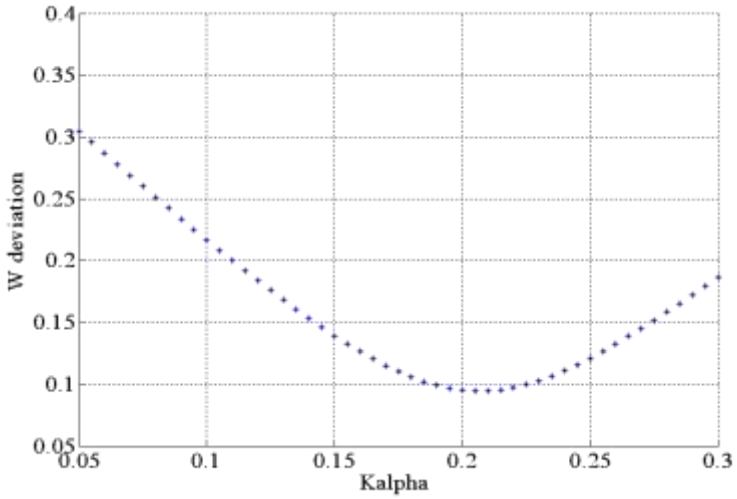

Fig 6.19: standard deviation of the calculated vertical wind component in respect with different angle of attack coefficients

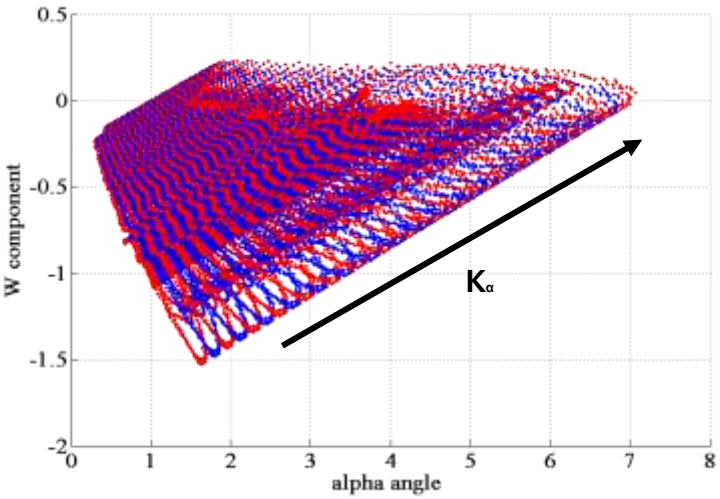

Fig 6.20: variation of the vertical wind component in respect with variation in angle of attack, for different angle of attack coefficients

Figure 6.20 shows how the vertical wind trend that goes to be straight while the *Kalpha* goes towards the optimum value, is also possible to see how the standard deviation diminish (figure 6.21 shows the vertical wind plume for *Kalpha*=0.205. From the figure 6.21 can be checked if the calibration is well done, in fact as we told before the rule of thumb criterion for acceptable calibration of the system is that peak-to-peak variation in the vertical wind should be less than 10% the variation of the ground-relative aircraft velocity, the red line is the vertical aircraft velocity and for each oscillation we have that the rule of thumb is accomplisced..

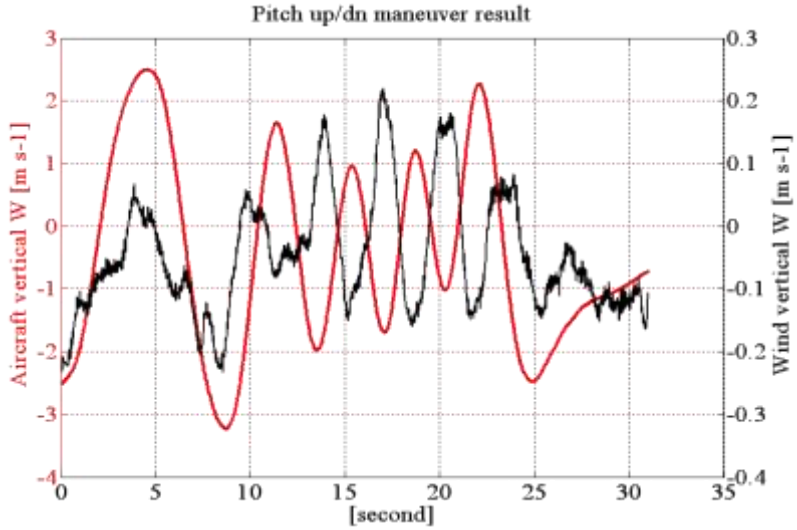

Fig 6.21: comparison between the vertical component of the aircraft ground speed and the calculated vertical wind component with the optimum angle of attack coefficient

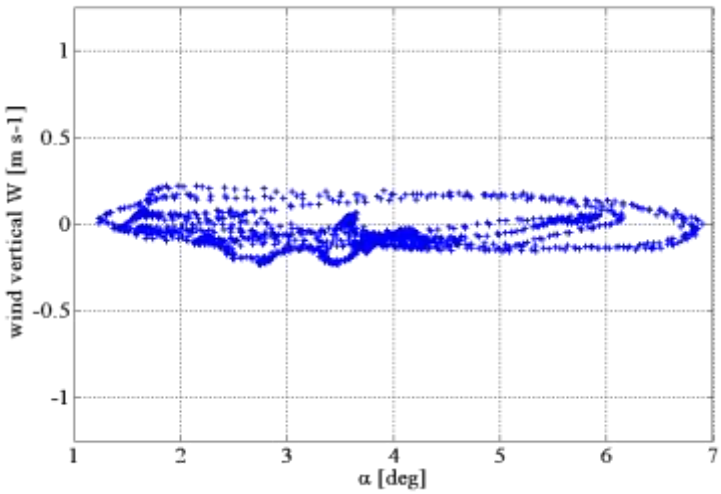

Fig 6.22: the computed vertical wind component Vs the angle of attack variation during the pitch oscillation maneuver

Yaw Left/Right

This maneuver also should be flown at constant pressure altitude. Depressing the left rudder pedal until the ball on the turn coordinator displaces approximately ¼ ball width, should change the heading of the aircraft. This is normal and should be allowed to continue as necessary. The deflection of ¼ ball should be maintained for 10 seconds, then with ball deflection as ½ ball width, and again with ball deflection approximately at ¾ ball width for 10 seconds each one. Finally, at full ball width. Altitude variance during this maneuver should be ±10 feet, airspeed variance should be ±1 knot, and bank angle variance should be ±2° during the entire maneuver.

The same procedure have to be repeated using right rudder pedal deflections.

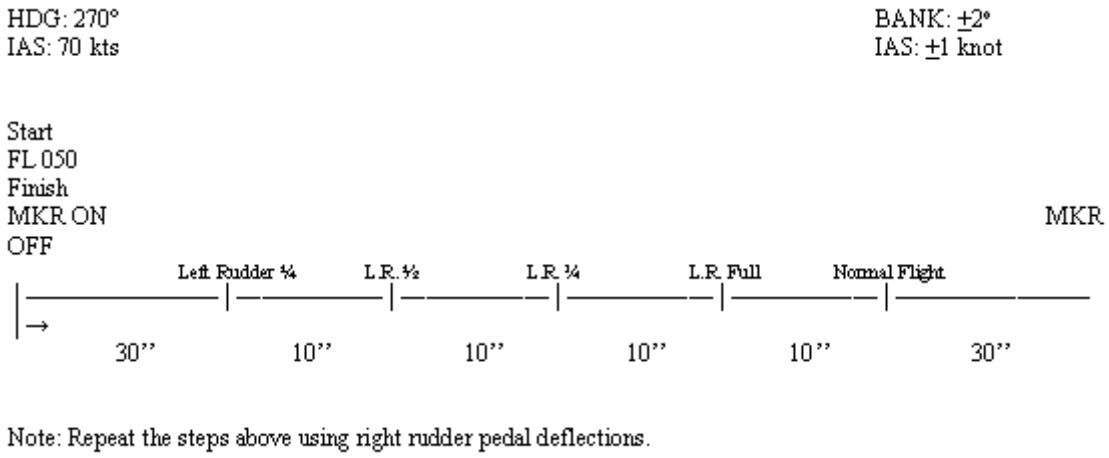

Fig 6.23: The yaw left/right maneuver procedure

On the "*yaw left/right*" manuever is calculated the optimum *"Kbeta"* coefficient, forcing the variance of the calculated horizontal wind magnitude and direction to the minimum.

Figure 6.24 shows the performed maneuver. In figure 6.25 are reported the standard deviation for the wind magnitude and direction versus the kbeta calibration factor. The best value found is of 0.19. Figures 6.26 and 6.27 show how the time series of the wind speed and direction rotate at the variation of kbeta, and how the deviation standard diminish.

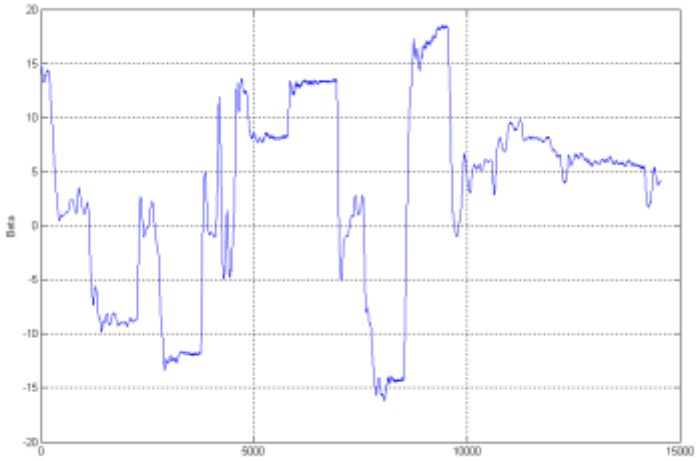

Fig 6.24: the sideslip angle during the maneuver

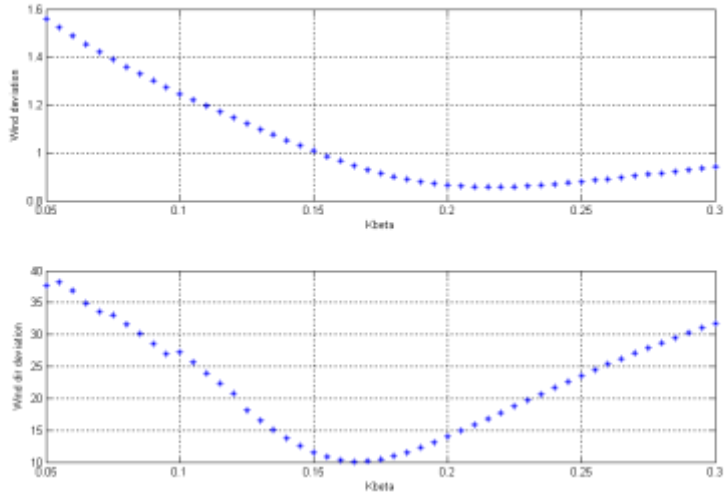

Fig 6.25: standard deviation of the magnitude and direction wind Vs the calibration factor Kbeta

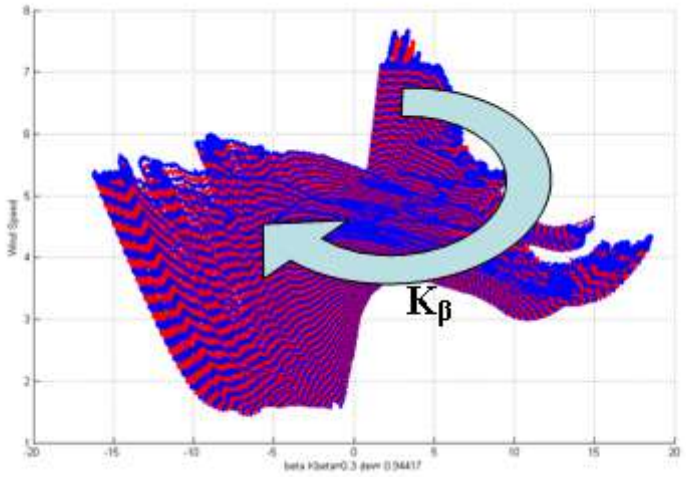

Fig 6.26: variation of the wind speed(y-axes) respect to variation in kbeta

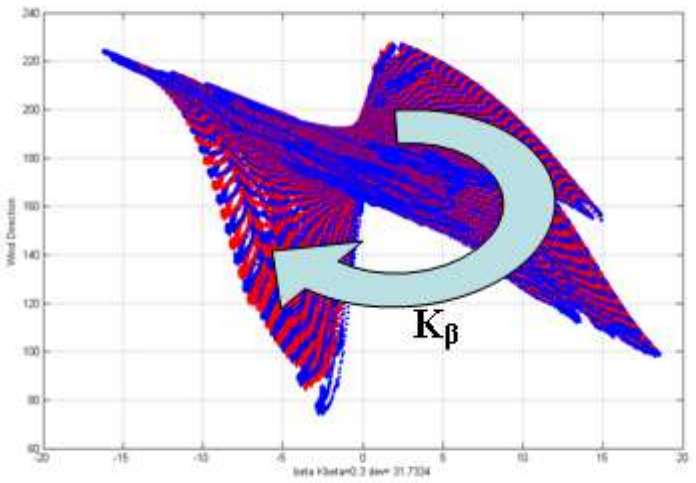

Fig 6.27: variation of the wind direction (y-axes) respect to variation in kbeta

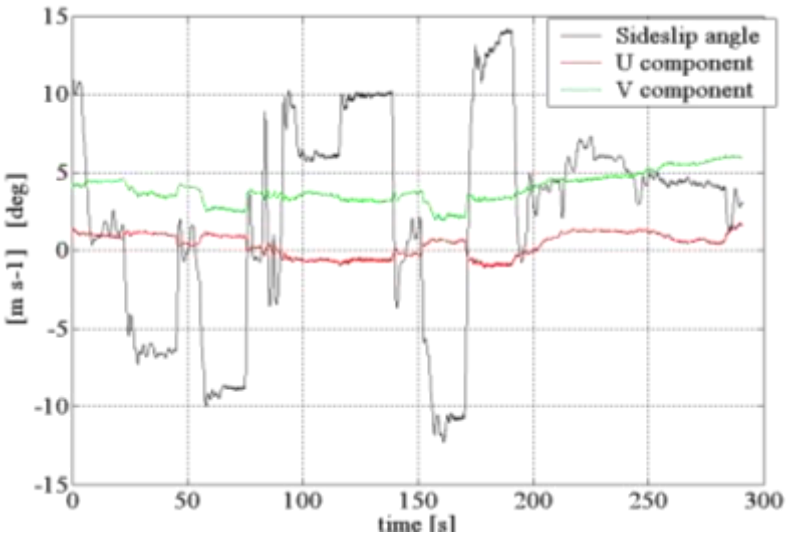

Fig 6.28: variation of the wind speed regards kbeta

In figure 6.28 are showed the residual error on the north and east component after the calibration.

Wind Circle

This maneuver should be flown at constant pressure altitude. Roll the airplane into a left standard rate turn and establish and maintain 70 KIAS. Maintain the condition through 360°. Continue the left turn through another 45-90°, roll the plane back to the right and repeat the procedure for a turn to the right. Altitude variance during this maneuver should be ±10 feet, airspeed variance should be ±1 knot, bank angle variance should be ±2°, and the turn rate variance should be held to a minimum as much as possible during the entire maneuver.

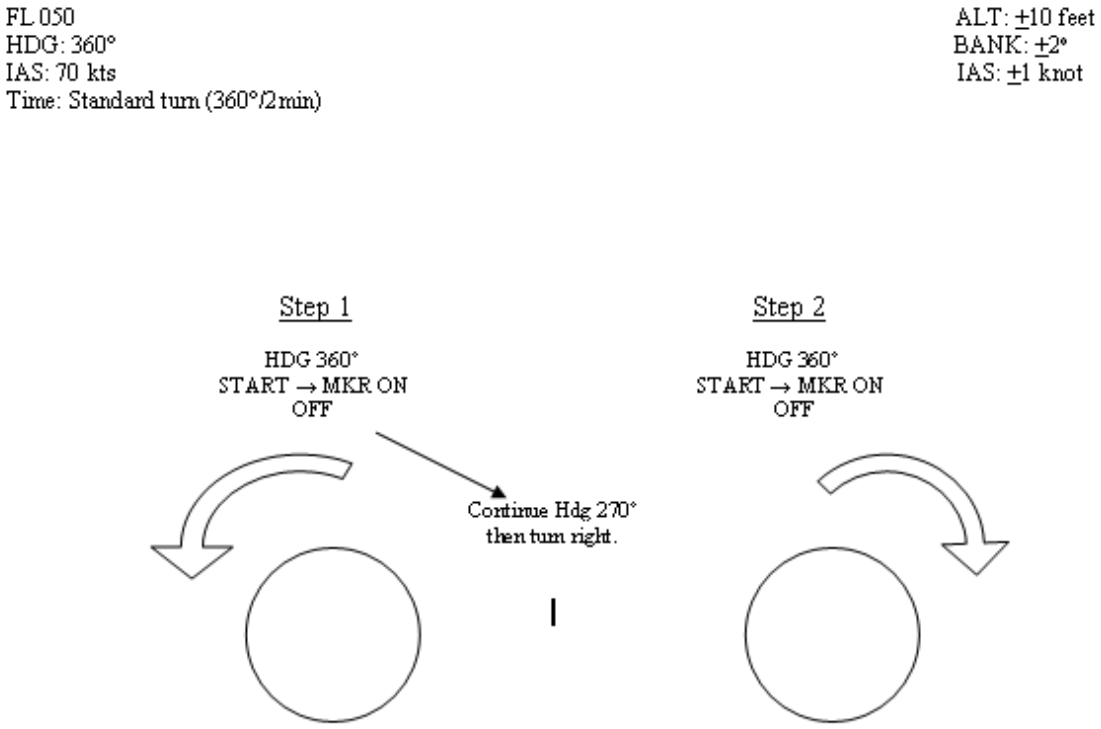

Fig 6.28: wind circle maneuver procedure

With the wind circle maneuver the performance of the horizontal wind component calibration factors can be tested.

5.2 Calculation of the wind vector using the M2AV

5.2.1 Introduction

The meteorological mini UAV 'M2AV ' was developed at the Institute of Aerospace Systems (ILR = Institut fur Luft- und Raumfahrtsysteme) at the Technical University of Braunschweig and build in cooperation with Mavionics GmbH, Braunschweig, Germany. The M2AV is controlled by an on-board autopilot system which communicates with a ground station (laptop PC) for the exchange of measured data and flight mission updates like new way-points. The meteorological sensors are mounted on a nose boom and consist of two temperature sensors, a humidity sensor and a five-hole probe (5HP). A GPS receiver and an inertial measurement unit (IMU) are on-board to measure the inertial velocity and the attitude angles. The first meteorological performance was during the LAUNCH-05 field experiment at the Meteorological Observatory Lindenberg (MOL) of the German Meteorological Service (DWD) (Spieß et al., 2007). Temperature and humidity measurements were compared with several remote-sensing systems and tower measurements. Since the LAUNCH-05 experiment the wind vector measurement has improved. A K´alm´an filter is used to couple both GPS and inertial navigation systems (INS) (Winkler and V¨orsmann, 2007). Combined with the measurement data from the 5HP, the M2AV is capable of calculating the mean and the turbulent wind vector with 40 Hz resolution corresponding to a spatial resolution of 55 cm.

5.2.2 Wind vector

The wind measurement by airborne systems is challenging. High resolution and thus fast and accurate sensors are needed to determine the attitude, position and the velocity of the aircraft relative to the earth, and the airflow at the nose of the fuselage with high accuracy.
The wind Wg defined in geodetic coordinate system is the vector difference between the inertial velocity Vg and the true airspeed Ua (neglecting the small lever-arm to the 5HP):

$$\mathbf{W}_g = \mathbf{V}_g + \mathbf{M}_{gb} \cdot \mathbf{M}_{ba} \cdot \mathbf{U}_a \qquad (1)$$

with the matrix Mba to transform the true airspeed from aerodynamic (index 'a') into body (index 'b') coordinates, and Mgb for the transformation into the geodetic coordinate system (index 'g').

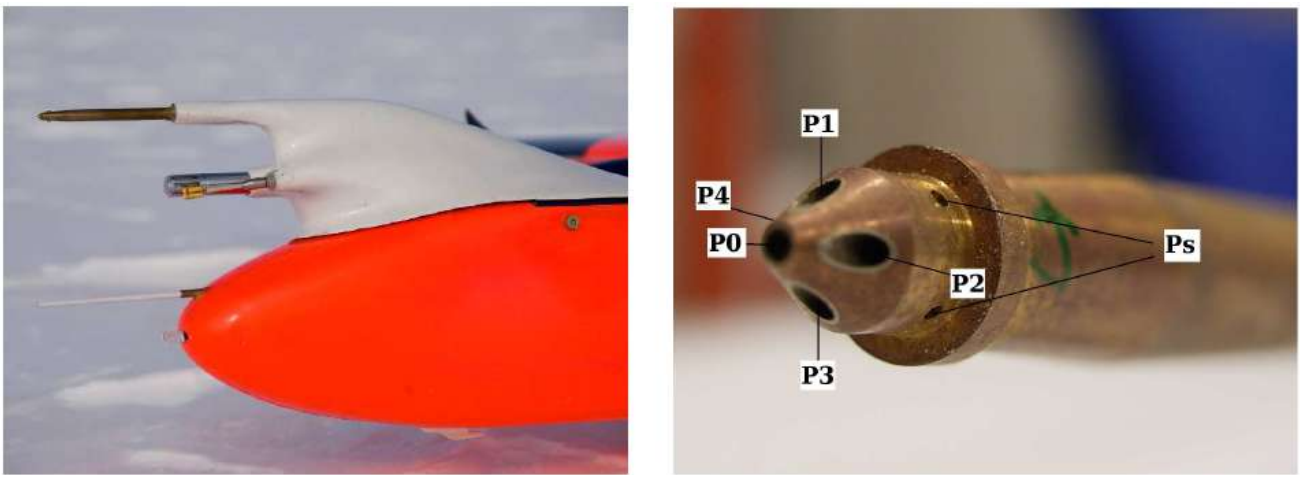

Figure 1: *Left: The measurement nose. Right: The 5HP with a diameter of 6 mm. The 4 smaller circumferential holes (only 2 visible) are the static pressure ports.*

To obtain all components of (1) in the geodetic coordinate system, two coordinate transformations have to be applied. First, the true airspeed vector Ua as measured in the aerodynamic coordinate system has to be transformed into the body coordinate system of the aircraft using the transformation according to Boiffier (1998), Lenschow (1986) and Axford (1968)

$$\mathbf{U}_b = \mathbf{M}_{ba} \cdot \mathbf{U}_a = \frac{|\mathbf{U}_a|}{D} \cdot \begin{bmatrix} 1 \\ \tan\tilde{\beta} \\ \tan\tilde{\alpha} \end{bmatrix} \qquad (2)$$

with a normalization factor

$$D = \sqrt{1 + \tan^2\tilde{\alpha} + \tan^2\tilde{\beta}} \qquad (3)$$

and the angles ˜ , ˜ (measured by the 5HP in flight) between the airflow and the x-axis and z-axis in body coordinate system, respectively. The norm |Ua| has to be calculated using the measured total air temperature Ttot, the static pressure p and the dynamic pressure q

$$|\mathbf{U}_a|^2 = 2 \cdot c_p \cdot T_{\text{tot}} \cdot \left[1 - \left(\frac{p}{p+q}\right)^{\kappa}\right] \qquad (4)$$

with the poisson number = R/cp where R = 287 J · K−1 · kg−1 is the gas constant for dry air and cp = 1005 J · kg−1 · K−1 the specific heat for dry air.
Then, the flow vector Ub has to be transformed into the geodetic system using Mgb (Haering, 1990;

Leise and Masters, 1993; Boiffier, 1998). Finally the resulting Wg has to be transformed into the standard meteorological frame of reference, with the wind components u, v and w (east-, north- and upwards, respectively, Lenschow 1986),

$$
\begin{aligned}
u = v_g = v_{Ag} - |\mathbf{U}_a| D^{-1} \Big[& (\cos\Theta \cdot \sin\Psi) + \tan\tilde{\beta} \cdot (\sin\Phi \cdot \sin\Theta \cdot \sin\Psi + \cos\Phi \cdot \cos\Psi) \\
& + \tan\tilde{\alpha} \cdot (\cos\Phi \cdot \sin\Theta \cdot \sin\Psi - \sin\Phi \cdot \cos\Psi) \Big] \quad , \\
v = u_g = u_{Ag} - |\mathbf{U}_a| D^{-1} \Big[& (\cos\Theta \cdot \cos\Psi) + \tan\tilde{\beta} \cdot (\sin\Phi \cdot \sin\Theta \cdot \cos\Psi - \cos\Phi \cdot \sin\Psi) \\
& + \tan\tilde{\alpha} \cdot (\cos\Phi \cdot \sin\Theta \cdot \cos\Psi + \sin\Phi \cdot \sin\Psi) \Big] \quad , \\
w = -w_g = -w_{Ag} + |\mathbf{U}_a| D^{-1} \Big[& (-1 \cdot \sin\Theta) + \tan\tilde{\beta} \cdot (\sin\Phi \cdot \cos\Theta) \\
& + \tan\tilde{\alpha} \cdot (\cos\Phi \cdot \cos\Theta) \Big] \quad ,
\end{aligned}
\tag{5}
$$

,with inertial velocity vector Vg = (uAg, vAg,wAg) and the Euler (attitude) angles pitch □, true heading
□ □and roll □.

5.2.3 Calibration of the airflow angles

The calibration of the 5HP was performed at the Pfleiderer institute (Technical University Braunschweig), which provided an open wind tunnel capable of wind velocities up to 100 m s−1. The 5HP was mounted on the M2AV fuselage nose and calibrated at an airflow velocity of 22 m s−1 and at predefined airflow angles □ □and □ □between −20◦ and +20◦. The measurement uncertainty of the wind tunnel velocity was 0.7% ≈ 0.2 m s−1 (for the specified velocity of 22 m s−1). The airflow angles were varied manually during the calibration with an uncertainty of 0.2◦.
These wind tunnel angles □ □and □ □are related to the airflow angles ˜ □ □and ˜□ □(Boiffier, 1998) used for the wind calculation (5):

$$
\begin{aligned}
\tilde{\alpha} &= \alpha \quad , \\
\tilde{\beta} &= \arctan\left(\frac{\tan\beta}{\cos\alpha}\right)
\end{aligned}
\tag{6}
$$

The 5HP has five total pressure ports on its conical head and four static pressure ports downstream the head (Fig. 1). Five differential pressures are measured: the difference between the central hole and

each of the four remaining total pressure ports (ΔP_{01}, ΔP_{02}, ΔP_{03}, ΔP_{04}) and the difference between the static pressure and the central hole (ΔP_{0s}). These measurements are used to determine a total pressure difference (Sasongko, 1997):

$$\Delta P = \left[\frac{1}{5}\sum_{i=0}^{4}\left(P_i - \frac{1}{5}\sum_{j=0}^{4}P_j\right)^2\right]^{\frac{1}{2}} + \left[P_0 - \frac{1}{4}\sum_{i=1}^{4}P_i\right] \quad , \tag{7}$$

which can be calculated by the individual pressure differences

$$\begin{aligned}\Delta P = \Bigg[\frac{1}{125}\Big((\Delta P_{01}+\Delta P_{02}+\Delta P_{03}+\Delta P_{04})^2 + (-4\cdot\Delta P_{01}+\Delta P_{02}+\Delta P_{03}+\Delta P_{04})^2 \\ +(\Delta P_{01}-4\cdot\Delta P_{02}+\Delta P_{03}+\Delta P_{04})^2 + (\Delta P_{01}+\Delta P_{02}-4\cdot\Delta P_{03}+\Delta P_{04})^2 \\ +(\Delta P_{01}+\Delta P_{02}+\Delta P_{03}-4\cdot\Delta P_{04})^2\Big)\Bigg]^{\frac{1}{2}} + \tfrac{1}{4}(\Delta P_{01}+\Delta P_{02}+\Delta P_{03}+\Delta P_{04}) \quad .\end{aligned} \tag{8}$$

Dimensionless pressure coefficients k_α and k_β are defined using ΔP and the measured differential pressures

$$k_\alpha = \frac{\Delta P_{01} - \Delta P_{03}}{\Delta P} \quad , \tag{10}$$

$$k_\beta = \frac{\Delta P_{02} - \Delta P_{04}}{\Delta P} \quad . \tag{11}$$

To calculate the airflow angles and the dimensionless coefficient k_q for the dynamic pressure, three functions were defined

$$\begin{aligned}\alpha &= f_1(k_\alpha, k_\beta) \quad , \\ \beta &= f_2(k_\alpha, k_\beta) \quad , \\ k_q &= f_3(k_\alpha, k_\beta) \quad ,\end{aligned} \tag{11}$$

with the general calibration polynomial form (11th order for both m and n) for f_x (x = 1,2 or 3)
according to Bohn and Simon (1975)

$$f_x(k_\alpha, k_\beta) = \sum_{i=0}^{m} (k_\alpha)^i \left[\sum_{j=0}^{n} X_{ij} (k_\beta)^j \right] \quad (12)$$

where $X_{i\,j}$ represents the coefficients for the angle of attack $a_{i\,j}$, sideslip angle $b_{i\,j}$ or dynamic pressure $q_{i\,j}$ for f_1, f_2 and f_3 respectively. The function (12) contains $m \cdot n$ unknown coefficients which can be determined with a system of $m \cdot n$ independent equations. This linear problem is solved by the least square method for all three functions (11) and returned the coefficients $a_{i\,j}$, $b_{i\,j}$ and $q_{i\,j}$.
The method enabled the determination of the airflow angles and the dynamic pressure coefficient k_q with the measurements of the 5HP. Finally the dynamic pressure q during flight is calculated

$$q = \Delta P_{0s} + \Delta P \cdot k_q \quad (13)$$

and used to calculate the true airspeed (4).

5.2.4 Determination of the attitude angles

The reliable determination of attitude, velocity and position of the aircraft is essential for wind identification.
With the M2AV this is achieved by an integrated navigation system consisting of a GPS and an INS. The INS calculates the position, velocity and attitude by a strapdown calculation of the accelerations and angular rates measured by the IMU. The GPS/INS system offers a significantly increased performance, compared to a INS only, due to the complementary characteristics of GPS and INS, where the latter assures the continuous availability of the attitude, velocity and position. The growth of navigation errors with time due to the low cost MEMS IMU is prevented by the use of aiding information provided by the GPS receiver. Figure 2 displays the navigation-filter architecture.
For the GPS/INS integration a discrete error state Kalman Filter was used (Gelb, 1989). Kalman filters are based on linear dynamic systems discretize in the time domain (Kalman, 1960). The system model uses the following discrete error-state vector: three position-, three velocity- and three attitude errors as well as three errors in the gyro sensor signal bias, three errors in the accelerometer signal bias, one error in the GPS receiver clock error and one error in the clock drift, which are in total 17 states. By processing GPS raw data (pseudo range, delta range and carrier phase), estimates of

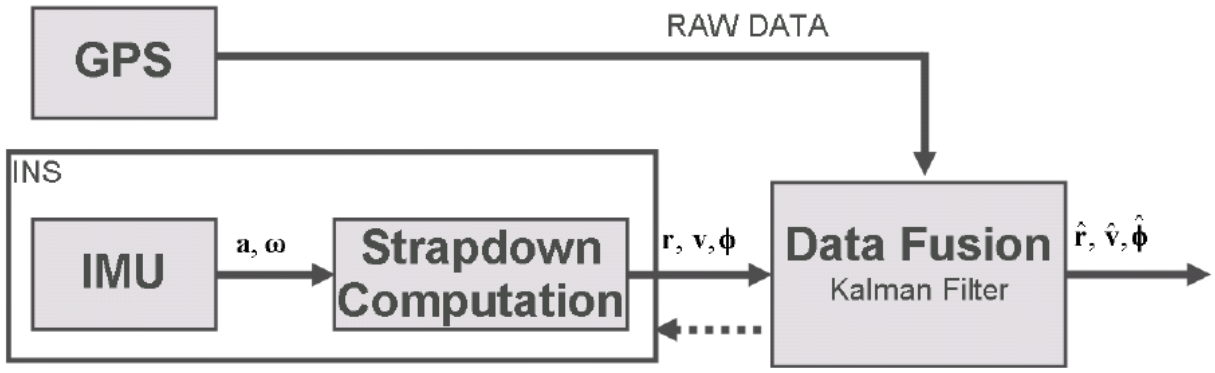

Figure 2: *Navigation filter structure where* **a** *and* ω *are the accelerations and the angular rates from the IMU,* **r**, **v** *and* ϕ *the position, velocity and attitude from the INS system. The position, velocity and attitude solution from the Kalman filter are defined as* $\hat{\mathbf{r}}$, $\hat{\mathbf{v}}$ *and* $\hat{\phi}$.

the error-state vector are made which corrects the full states of the navigation system. The GPS receiver measures the delay of the satellite signal and calculates the distance to the satellite, which is called the pseudo range. The delta range is the velocity of the GPS receiver relative to the satellite calculated via Doppler shift of the carrier wave. The receiver gives also the phasing of the carrierwave. This method of aiding is called tightly coupled (Wendel and Trommer, 2004). Furthermore, with such a filter the INS can still be aided by GPS when there are less than four visible satellites.

A tightly-coupled GPS/INS filter usually processes pseudo ranges and delta ranges. Based on the method used by Farrell (2001) and van Graas and Farrell (2001), the delta ranges can be replaced by time-differenced carrier phases and used for the M2AV navigation (Winkler and V¨orsmann, 2007). It was proofed that the filter with time-differenced carrier phase achieved a better velocity and attitude accuracy than the filter using delta-ranges. The method allows using the high measurement accuracy of the carrier phase without solving the integer ambiguities. Compared to a delayed state K´alm´an filter (which would be commonly used in such case) this method does not induce additional crosscorrelation between measurements at one epoch.

5.2.5 Wind vector calibration

The wind vector (5) calculated from airborne measurements is very sensitive to errors in the input parameters. The first M2AV data sets were measured in both convective and neutral stratification.
During these flights the mean vertical wind was expected to be nearly zero, but the actually measured w showed a deviation of a few m s−1. The mean horizontal wind components were assumed to be constant during the entire flight, however both measured u and v changed stepwise depending on the flight direction.

The impact of sensor errors on the wind calculation

A simple error estimation (V¨orsmann, 1985) was made in order to identify the parameters causing the above described systematic errors in the horizontal and vertical wind components. To quantify the errors a reference state for the M2AV was defined (Tab. 1): a typical airspeed of 20 m s−1 , small airflow angles and Euler angles (0.02 rad), a vertical velocity of 1 m s−1 and the horizontal velocity

Table 1: *Error estimation; differences Δu, Δv and Δw between the reference and erroneous wind components.*

Parameter	Input	Δu	Δv	Δw
Ψ	$0 \ldots 2\pi$ rad	$0.4 \cos\Psi$	$-0.4 \sin\Psi$	0
Θ	0.02 rad	$-4 \cdot 10^{-3} \sin\Psi$	$-4 \cdot 10^{-3} \cos\Psi$	-0.4
Φ	0.02 rad	$-8 \cdot 10^{-3} \cos\Psi$	$-8 \cdot 10^{-3} \sin\Psi$	$-8 \cdot 10^{-5}$
α	0.02 rad	$-4 \cdot 10^{-3} \sin\Psi$	$-4 \cdot 10^{-3} \cos\Psi$	0.4
β	0.02 rad	$0.4 \cos\Psi$	$-0.4 \sin\Psi$	0
$\mathbf{U}_a$	20 m s^{-1}	$0.5 \sin\Psi$	$0.5 \cos\Psi$	0
v_{Ag}	$20 \cdot \sin\Psi$ m s^{-1}	-0.5	0	0
u_{Ag}	$20 \cdot \cos\Psi$ m s^{-1}	0	-0.5	0
w_{Ag}	1 m s^{-1}	0	0	-0.5

components were set to 20 m s−1 depending on the flight direction. Proximate, the reference wind components (uref, vref and wref) were calculated as a function of the true heading (0. . .360◦).
The effect of every individual parameter (nine parameters in total) was determined by defining typical measurement errors with values of 0.5 m s−1 for the velocities and 0.02 radian (≈ 1◦) for the angles.
These errors were added to the reference states and used to calculate the erroneous wind components (u_{err}, v_{err} and w_{err}), for every separate parameter.

Table 1 shows the differences Δu, Δv and Δw between the reference and erroneous wind components.

Except for the inertial velocity components, the error estimations for u and v depended on the flight direction (Tab. 1). An error in the sideslip angle or the true heading resulted in an erroneous u component in north (0◦) or south (180◦) flight direction and an erroneous v component in east (90◦) or west (270◦) flight direction. A true airspeed error also affected both u and v significantly dependingon the flight direction. The largest deviation of w was caused by the errors in Θ, α and the vertical velocity w_{Ag}, independent of the flight direction.

Assuming that the separation of the IMU origin and the 5HP is negligible, the spheric coordinates of a wind vector measured by the the 5HP in the IMU coordinate system (defined as the body coordinate system) are $\Delta\Phi'$, $\Delta\Theta'$ and $\Delta\Psi'$, corresponding to rotations about the x-, y- and z-axis, respectively.

To transform the measured true airspeed in geodetic coordinates, the Euler angles (measured by the INS/GPS) have to be corrected by these unknown angles $\Delta\Phi'$, $\Delta\Psi'$ and $\Delta\Theta'$. As shown by the error estimation, the error in Φ had an insignificantly effect on the computed u, v and w, therefore $\Delta\Phi'$ was neglected and set to zero. While the remaining biases can not be measured, a flight strategy was chosen to determine $\Delta\Theta'$ and $\Delta\Psi'$.

The dynamic pressure (and the true airspeed) was calculated using the wind tunnel calibration polynomials.

Unfortunately, the wind tunnel was too small for the complete aircraft and therefore the

calibration setup was reduced to a shorter fuselage. The wing of the aircraft including both engines and the full body were not taken into account and therefore the actual flow distortion during flight, was not included in the calibration. This effect can only be corrected by a new calibration in a larger wind tunnel or by an in-flight calibration. Since a new calibration in a larger wind tunnel is currently not feasible, the aerodynamic effect especially of the wings and the propulsion are approximated by a correction factor f_{u_a} of the true airspeed.

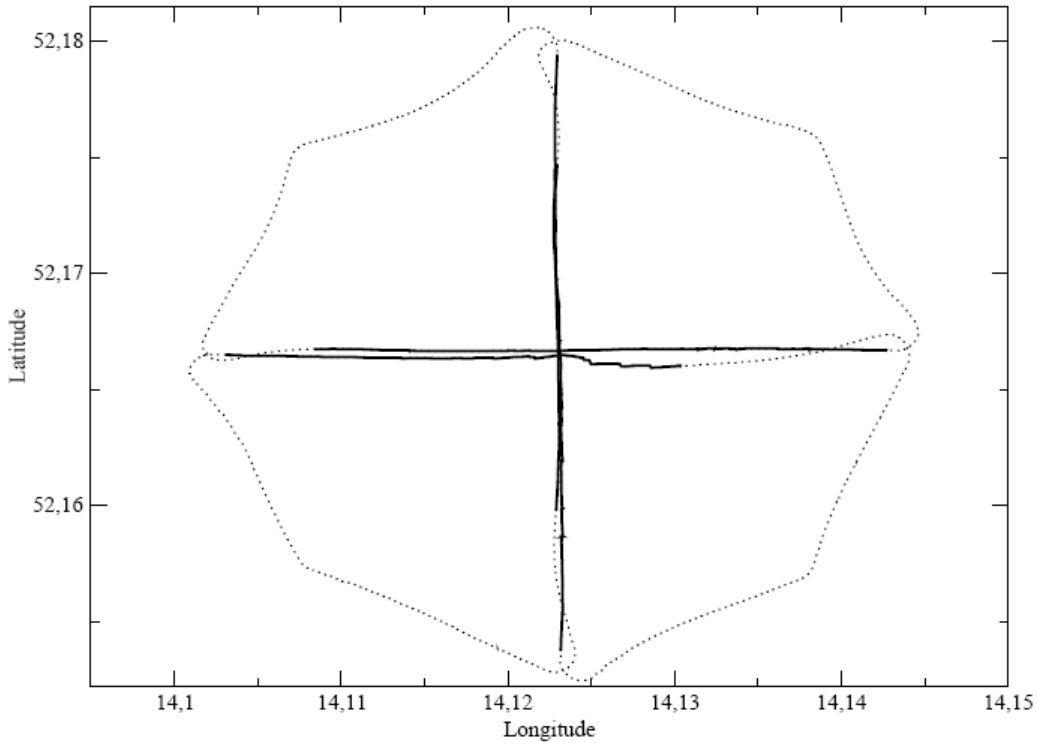

Figure 3: *Star flight pattern performed on 1 August, 2007, the dotted line represents the complete flight, the solid lines the horizontal legs used for the in-flight calibration.*

In-flight wind calibration

In total three correction factors, $\Delta\Psi'$, $\Delta\Theta'$ and f_{U_a} have to be determined. The appropriate flight
pattern for the in-flight calibration is a star pattern (Fig. 3). The ideal atmospheric conditions are no large turbulent transport, a constant mean horizontal wind and a mean vertical wind near zero. For every straight horizontal leg the mean values ($\mathbf{U}a$,α,β ,Θ,Ψ,Φ,*uAg*, *vAg*,*wAg*, uncorrected) will be calculated from the measured time series. These mean values will be used to calculate the mean wind vector using equation (5) which is supplemented by the unknown correction factors. The following parameter are replaced in (5)

$$\begin{aligned} \Theta &\Rightarrow \overline{\Theta} + \Delta\Theta' \quad , \\ \Psi &\Rightarrow \overline{\Psi} + \Delta\Psi' \quad , \\ \mathbf{U}_a &\Rightarrow \overline{\mathbf{U}}_a \cdot f_{\mathbf{U}_a} \quad , \end{aligned} \tag{14}$$

where Θ, Ψ and $\mathbf{U}_a$ are the mean values of the pitch angle, true heading and the true airspeed, respectively.

The assumptions that the mean horizontal wind components are actually identical on a round trip and the mean vertical wind is close to zero, leads to the following set of equations

$$\begin{aligned} \overline{u}^n - \overline{u}^s = 0, \quad \overline{v}^n - \overline{v}^s = 0 \quad , \\ \overline{u}^w - \overline{u}^e = 0, \quad \overline{v}^w - \overline{v}^e = 0 \quad , \\ \overline{w}^n = \overline{w}^s = \overline{w}^w = \overline{w}^e = 0 \quad , \end{aligned} \tag{15}$$

where *n*, *s*, *w* and *e* indicate north, south, west or east flight direction.
The unknown parameters $\Delta\Psi'$, $\Delta\Theta'$ and f_{Ua} were then calculated from (5) complemented with (14) and (15) using the Levenberg-Marquardt least squares fit method (Press et al., 1992).

5.2.6 References

Axford, D. N., 1968: On the accuracy of wind measurements using an inertial platform in an aircraft,
and an example of a measurement of the vertical mesostructure of the atmosphere. *J. Appl. Meteor.*,
7, 645–666.
Bohn, D. and H. Simon, 1975: Mehrparametrige approximation der eichr¨aume und eichfl¨achen von
unterschall- bzw. ¨uberschall-5-loch-sonden. *ATM, Bd. 42*, **3**, 31–37.
Boiffier, J.-L., 1998: *The Dynamics of Flight – the Equations*.Wiley, Chichester, UK, 353 pp.
Farrell, J. L., 2001: Carrier phase processing without integers. *the Institute of Navigation 57th Annual*
Meeting, ION, Albuquerque, NM, 423–428.
Gelb, A. H., 1989: *Applied Optimal Estimation*. The M.I.T.. Press, Cambridge, MA, London.
Haering, E. A., 1990: Airdata calibration of a high-performance aircraft for measuring atmospheric
wind profiles. Tech. Mem. 101714, NASA, 24 pp.
K´alm´an, R. E., 1960: A new approach to linear filtering and prediction problems. *Trans. ASME, J.*
Basic Eng., **82**, 35–45.
Leise, J. A. and J.M.Masters, 1993: *Wind measurements from aircraft*.US Department of Commerce,
National Oceanic and Atmospheric Administration, Aircraft Operation Center, Miami, Florida,
USA, 166 pp.
Lenschow, D. E., 1986: *Probing the atmospheric boundary layer*. American Meteorological Society,
289 pp.

Press, W., B. Flannery, S. Teukolsky, and W. Vetterling, 1992: *Numerical recipes in C: The art of*
scientific computing. Cambridge University Press, 1020 pp.
Sasongko, H., 1997: *Rand- und Spaltstr¨omungen in stark gestaffelten Verdichtergittern aus schwach*
gew¨olbten Profilen. No. 1997-01 in ZLR-Forschungsbericht, Technische Universit¨at Braunschweig.
Spieß, T., J. Bange, M. Buschmann, and P. V¨orsmann, 2007: First application of the meteorological
mini-UAV 'M2AV'. *Meteorol. Z. N. F.*, **16 (2)**, 159–169.
van Graas, F. and J. L. Farrell, 2001: GPS/INS - a very different way. *the Institute of Navigation 57th*
Annual Meeting, ION, Albuquerque, NM, 715–721.
V¨orsmann, P., 1985: Ein Beitrag zur bordautonomenWindmessung. Ph.D. thesis, Techn. Univ. Braunschweig,
Germany, 117 pp.
Wendel, J. and G. F. Trommer, 2004: Tightly coupled GPS/INS integration for missile applications.
Aerospace Science and Technology, **8**, 627–634.
Winkler, S. and P. V¨orsmann, 2007: Multi-sensor data fusion for small autonomous unmanned aircraft.
Eurpean Journal of Navigation, **5 (2)**, 32–41.

5.3 Using "Rodi" maneuvers to calibrate gust probe measurements from an Instrumented Aircraft

5.3.1 Introduction

The following briefly outlines the philosophy and corresponding procedures used to calibrate the wind/gust system on the University of Wyoming King Air aircraft. Note, this work was developed by Al Rodi at UW and differs from the "standard" techniques of utilizing "Lenschow" maneuvers for calibrating airborne wind systems.

5.3.2 Philosophy

The basic philosophy for this calibration procedure centers on the idea that there exist errors in the measurement system (such as misalignment between the coordinate systems) or departures from theoretical values for relationships between flow fields around the gust probe and pressure port measurements. This is similar for nearly all calibration methods, and calibration factors are introduced to account for the errors or departures, typically factors for attitude angle offsets, factors for relationships between flow angles (alpha and beta) and differential pressure

measurements, and factors for relationships between dynamic pressure and airspeed.

Unlike other, more "typical" methods for calibration, there is no attempt to isolate inputs using a maneuver. Rather, an attempt is made to vary as many inputs as possible at a single time. In doing so, mis-calibrations (or deviations from theory, or errors in alignment) will result in an over increase in the variance seen in the computed three-dimensional wind vector. By using a multi-variate numerical scheme to adjust calibration coefficients, minimizing some function of the wind vector or tke, or some such, should allow one to determine the optimal set of calibration coefficients for the system.

5.3.3 Method

The calibration procedure begins with in-flight maneuvers. The maneuvers consist of two sets of circles conducted at "standard rate" (~25 degree bank). Circles alone are very efficient at teasing out errors due to misalignment in heading and/or airspeed. Because both sets of circles consist of one circle right and another circle left, misalignment in roll angles also directly result in errors of the calculated wind vector. Each set of circles is modified by adding an aircraft maneuver. During one set of circles the pilot induces side slip by using rudder. Roughly ½ to ¾ ball side slippage, relatively smoothly through the circle. In doing so, the result induces both sideslip (beta, primary) and attack (alpha, secondary) variations during the turn. Because the aircraft is banked, the sideslip feeds into both the horizontal and vertical wind calculation. During the second set of turns, the airspeed is varied around the circle such that as the turn is established, the pilot reduces power to attempt to hit minimum speed at roughly 180 degrees through the turn, then increases power to hit maximum speed at the complete of the circle. Doing so allows measurements over a range of airspeeds as well as a full range of attack angle (alpha).

The appropriate calibration coefficients, chosen in our case to include first order coefficients for attack angle, side-slip angle, and airspeed, and (constant) offset angles for the attitude angles (pitch, roll and heading), are determined through a numerical iterative process. Our process uses matlab routines to solve the system of equations that are used to compute the wind. In this manner the variation of the wind vector (during the maneuver) is forced to a minimum, the resulting calibration coefficients are thusly determined.

Similar methodology can be based on forcing some function described by the 3D wind vector to be minimized. One may choose to minimize tke, variance of wind

vector, or something like {w*wndspd}, the appropriate choice of the function to be minimized can be decided upon by the user.

5.4 Calibration process for the ATR-42 aircraft

Marie Lothon (Laboratoire d'A´erologie, Toulouse), Philippe Nacass (M´et´eo-France), Gilles Vergez (SAFIRE-M´et´eo-France, Francazal)

March 5, 2008

This is a brief summary of the method used by SAFIRE for the calibration of the sensors used to measure the air motion at high rate.

5.4.1 Introduction

The velocity of the air is obtained with the classical way by substracting the airplane velocity realtive to the ground from the air velocity relative to the plane. The first is measured by an INS (ULYSS-45), the latter is measured by a radome gust probe.

Thus, the variables that need to be calibrated are: the static pressure, the side slip angle, and he attacke angle.

A picture of the ATR-42 is given below.

The calibrations should be made before each field campaign that lasts more than one month, or once a year, and each time there is any change, move or failure in sensors, transducers, ports, radome, acquisition system....

5.4.2 Static pressure

Method: "Tower fly-by"

.The aircraft flys over a tower or along the take off and landing runway, with measurement of pressure, temperature, humidity and wind made at the ground and a few tens of meters above, using a tower or a tethered balloon.
The static error Pcor is the difference between the static pressure measured at the aircraft port PS and the pressure measured at the ground-based point, corrected for the altitude of the flight if

Figure 1: The ATR-42 research aircraft

needed (with Laplace formula, that assumes a standard atmosphere). The height of the aircraft is measured with an altimeter onboard.

Several fly-bys are made at different true airspeed, from the lowest to the highest airspeed of the airplane envelop, and including one fly-by at the cruise airspeed. Example for the ATR: 7 legs at 200 ft at 180 kt (cruise), 140 kt (mini), 230 kt (maxi), 160, 210, 140, 230 kt.

The static error is then plotted as a function of the dynamical pressure Q. This give the coefficient of calibration of the static pressure measured at the aircraft static port as a function of the dynamic pressure.

$$P_{cor} = c_1 + c_2\, Q,$$

$$PSC = PS - P_{cor},$$

$$QC = Q + P_{cor},$$

where PSC and QC are the calibrated static pressure and corrected dynamic pressure.

Recommendations:

- The maneuver must be made with manual control, because of the low height.
- The pressure measurement at the ground must be of high accuracy (_ 0.2 hPa).

• It is useful to make the first acquisition of both pressure measurements (ground and aircraft)

at the ground before takeoff.

• The same maneuver can be used for the static temperature calibration. The temperature

static error is then plotted as a function of U2

a /(2Cp) where Ua is the true airspeed.

• Favourable conditions are low wind, stationary pressure, non-turbulent airmass, no low clouds. Cloudy mornings avoid turbulence, fast changes and large gradients close to the ground.

5.4.3 Attack angle

Principle:

The method assumes no difference between the pitch and the attack angle when there is no vertical motion of the aircraft relative to the air. In such conditions, the attack angle can be calculated from the measurement of pitch. A range of attack angles is explored by flying at different airspeeds (from 140 kt to 230 kt for the ATR-42).

The calculated attack angle is then plotted as a function of the measured attack angle, that is as a function of the differential pressure _P_ and dynamic pressure QC:

$$\alpha_{cal} = C_3 + C_4 * \Delta P\alpha/QC \qquad (2)$$

Recommendations:

• Favourable conditions are steady flow, with no turbulence and no vertical motion of the air.

This often requires to fly high.

• Automatic pilot may be used, depending on the flight height.

5.4.4 Sideslip angle

Principle:

During a specific reverse heading maneuver, the sideslip _ angle is calculated as a function of the ground speed horizontal components, drift, true heading, mean wind and true airspeed.

Several forced skids are flown at the cruise airspeed at different values of sideslip angle values, and in different directions relative to the mean wind: upwind, downwind and crosswind.

The mean wind is estimated by flying a few drifting circles prior to the maneuver. The calculated sideslip angle is then plotted as a function of the measured sideslip angle, that is as a function of the differential pressure _P_ and dynamic pressure QC:

$$\beta_{cal} = C_3 + C_4 * \Delta P_\beta / QC \, . \qquad (3)$$

Recommendations:

• This maneuver requires uniform conditions, both in wind and thermodynamics.

• A measure of the pressure at the ground must be made before take off, along with along with

a ground reference measurement (like in the static pressure calibration).

6. List of participants

#	NAME	FIRT NAME	INSTITUTE	e-mail	Status
1	Bange	Jens	TUBS	j.bange@tu-bs.de	Present
2	Bitter	Mark	TUBS	mark.bitter@tu-bs.de	Present
3	Alfieri	Silvia	CNR ISAFoM	s.alfieri@isafom.cnr.it	Present
4	Bonnee	Wim	NLR	bonnee@nlr.nl	Present
5	Cremer	Mathias	TUBS	m.cremer@tu-bs.de	Present
6	Esposito	Marco	cosine Research	m.esposito@cosine.nl	Present
7	French	Jeff	WYM	jfrench@uwyo.edu	Present
8	Ger	Nielen	NLR	nielen@nlr.nl	Present
9	Jentik	Henk	NLR	jentink@nlr.nl	Present
10	Junkermann	Wolfgang	FZK	Wolfgang.Junkermann@imk.fzk.de	Not present
11	Lothon	Marie		lotm@aero.obs-mip.fr	Present
12	Magliulo	Enzo	CNR ISAFoM	v.magliulo@isafom.cnr.it	Present
13	Neninger	Bruno	METAIR	bruno.neininger@metair.ch	Present
14	Richener	Hans	ETHZ	hans.richner@ethz.ch	Present
15	Serrano Vargas	Oscar	INTA	serranovo@inta.es	Present
16	Smit	herman	Juelich	h.smit@fz-juelich.de	Not present
17	Van Den Kroonenberg	Alice	TUBS	a.kroonenberg@tu-bs.de	Present
18	Kalogiros	John	NOA	jkalog@meteo.noa.gr	Present
19	Donnarumma	Paolo	CNR ISAFoM	p.donnarumma@isafom.cnr.it	Present
20	Villagrasa	Daniel Martínez	Balearic University	dani.martinez@uib.cat	Present
21	Kraft	Stefan	cosine Research	s.kraft@cosine.nl	Present
22	Sabbatini	Massimo	ESA	Massimo.sabbatini@esa.int	Present

7. Turbulence References

As requested during both the first and the second turbulence Expert Working Group meetings, a list of the most useful references papers is included, with the intent to help young scientists that approach the topic.

Axford, D. N., 1968: On the Accuracy of Wind Measurements Using an Inertial Platform in an Aircraft, and an Example of a Measurement of the Vertical Mesostructure of the Atmosphere, *J. Applied Meteorology, **7**, 645-646.*

Bhattacharjee, J.K, 1994,"Screening approximation and the Kolmogorov spectrum of homogeneous isotropic turbulence" J. Phys. A: Math. Gen. 27 L347-L350 doi:10.1088/0305-4470/27/10/008

Boghel, W., and R.Baumann, 1991: Test and calibration of the DLR Falcon wind measuring system by maneuvers. *J. Atmos. Ocean. Technol., **8**, 5-18.*

Brown, E. N., C. A. Friehe, and D. H. Lenschow, 1983: The use of pressure fluctuations on the nose of an aircraft for measuring air motion. *J. Climate Appl. Meteorol.,* **22,** 171-180.

Cooper, W. A., and D. Rogers, 1991: Effects of airflow trajectories around aircraft on measurements of scalar fluxes. *J. Atmos. Oceanic Technol.,* **8,** 66–77.

Crawford, T. L., and R. J. Dobosy, 1992: A sensitive fast-response probe to measure turbulence and heat flux from any airplane. *Bound.-Layer Meteor.,* **59,** 257–278.

---------- , T.L., McMillen, R.T., Dobosy, R.J., MacPherson, I., 1993. Correcting airborne flux measurements for aircraft speed variation. Boundary-Layer Meteorol. 66, 237–245.

---------- , and E. J. Dumas, 1996: Aircraft wind measurement considering lift-induced upwash. *Bound.-Layer Meteor.,* **80,** 79–94.

Desjardins, R.L., MacPherson, J.I., Schuepp, P.H., Karanji, F., 1989. An evaluation of aircraft measurements of CO2, water vapour and sensible heat. Boundary-Layer Meteorol. **47**, 55–69

Dobosy, R. J., and T. L. Crawford, 1996: Accurate aircraft wind measurements using the global positioning system (GPS). *Proc. Conf. and Exhibition on Airborne Remote Sensing,* San Francisco, CA, ERIM International, 24–27.

Eckman, R. M., T. L. Crawford, E. J. Dumas, and K. R. Birdwell, 1999: Air-borne meteorological measurements collected during the Model Validation Program (MVP) _eld experiments at Cape Canaveral, Florida, in press as a NOAA Technical

Memorandum, NOAA Air Resources Laboratory, Atmospheric Turbulence and Diffusion Division, Oak Ridge, TN

Etkin, B., 1963: *Dynamics of Flight—Stability and Control.* Wiley and Sons, 519 pp.

Flēchard, C. R., R. L. Desjardins, J. I. MacPherson, T. Zhu, D. Wang, and E. Pattey, 2001: Measuring Trace Gas Fluxes on a Regional Scale Using Airborne Relaxed Eddy Accumulation, Proc. 11th AMS Symposiu

French, J. R., R. Johnson, S. Beard, and T. L. Crawford, 2004: Modification of an airborne gust probe for hurricane boundary layer research. *Proc. 26th Conf. On Hurricanes and* Tropical Meteorol. 332-333. Am. Meteorol. Soc., Boston, MA.

------- , Drennan, M., Zhang, A., Black, G., 2006: Turbulent fluxes in the hurricane boundary layer, I. momentum flux. Presented at *J. Atmospheric Science on 08-2006*

Gioli B., Franco Miglietta, Biagio De Martino, Ronald W.A. Hutjes, Han A.J. Dolman, Anders Lindroth, Marcus Schumacher, Maria Jose` Sanz, Giovanni Manca, Alessandro Peressotti, Edward J. Dumas, 2004. Comparison between tower and aircraft-based eddy covariance fluxes in five European regions. Agricultural and Forest Meteorology.

Hacker, J. M., and T. L. Crawford, 1999: The BAT probe: The ultimate tool to measure turbulence from any kind of aircraft (or sailplane). *J. Tech. Soaring,* **23:**2, 43-46.

Haering, E. A., Jr., 1992: Airdata calibration techniques for measuring atmospheric wind profiles. *J. Aircraft,* **29,** 632–639.

Horst, T.W., 1997. A simple formula for attenuation of eddy fluxes measured with first-order-response scalar sensors. Boundary - Layer Meteorol. 82, 219–233.

Khelif, D., S. P. Burns, and C. A. Friehe, 1999: Improved wind measurements on research aircraft. *J. Atmos. Ocean. Technol.,* **16,** 860-875

Lowson, R.P.,1979: A system for airborne measurement of vertical air velocity. *J.Appl.Meteor.,* **18**, 1363-1368.

Leach, B. W., and J. I. MacPherson, 1991: An application of Kalman filtering to airborne wind measurement. *J. Atmos. Oceanic Technol.,* **8,** 51–65.

Legrand, M., Pietras, C., Brogniez, G., Haeffelin, M., Khalil Abuhassan, N., and Sicari, M.,: A High-Accuracy Multiwavelength Radiometer for In Situ Measurements in the Thermal Infrared. Part I: Characterization of the Instrument *Journal of Atmospheric and Oceanic Technology*, Volume **17**, Issue 9 (September 2000) pp. 1203–1214.

-------, and , 1994: Comments on ''Correction of inertial navigation with Loran C on NOAA's P-3 aircraft.'' *J. Atmos. Oceanic Technol.,* **11,** 1048–1053.

Leise, J. A. and J. M. Masters, 1991: Wind measurement from aircraft, draft report, NOAA Aircraft Operations Center, Miami, FL.

Lenschow, D. H., 1972: The measurement of air velocity and temperature using the NCAR Buffalo aircraft measuring system. NCAR Tech. Note EDD-74, 39 pp. [Available from UCAR Communications, P.O. Box 3000, Boulder, CO 80307-3000.]

-------, 1986: Aircraft measurements in the boundary layer. *Probing the Atmospheric Boundary Layer,* D. H. Lenschow, Ed., Amer. Meteor. Soc., 39–55.

-------, E. R. Miller, and R. B. Friesen, 1991: A three-aircraft intercomparison of two types of air motion measurement systems. *J. Atmos. Oceanic Technol.,* **8,** 41–50.

MacPherson, J. I. and R. L. Desjardins, 1991: Airborne Tests of Flux Measurement by the Relaxed Eddy Accumulation Technique, 7th Symp. on Met. Observations & Instrumentation, 6-11, New Orleans.

-------, 1978: Wind tunnel and flight tests of temperature probes used on the NAE T-33 and Twin Otter atmospheric research aircraft. NRC Report NAE LTR-FR-62, 34 pp. [Available from Flight Research Laboratory, National Research Council, Ottawa, ON K1A 0R6, Canada.]

-------, 1985: Wind tunnel calibration of a PMS canister instrumented for airflow measurement. NRC Report NAE NAE-AN-32, 63 pp. [Available from Flight Research Laboratory, National Research Council, Ottawa, ON K1A 0R6, Canada.]

-------, 1990: Wind and flux calculations on the NAE Twin Otter. NRC Report NAE LTR-FR-109, 38 pp. [Available from Flight Research Laboratory, National Research Council, Ottawa, ON K1A 0R6, Canada.]

-------, 1993: Use of a wing-mounted airflow pod for airborne wind and flux measurement. Preprints, *Eighth Symp. on Meteorological Observations and Instrumentation,* Anaheim, CA, Amer. Meteor. Soc., 169–174.

-------, and D. Baumgardner, 1987: Studies of aircraft flow effects about wing-mounted PMS probes. Preprints, *Sixth Symp. on Meteorological Observations and Instrumentation,* New Orleans, LA, Amer. Meteor. Soc., 144–147.

Masters, J. M., and J. A. Leise, 1993: Correction of inertial navigation with Loran C on NOAA's P-3 aircraft. *J. Atmos. Oceanic Technol.,* **10,** 145–154.

NASA. NASA System Engineering Handbook. Washington D.C.: NASA, 1995.

Rosemount, 1981: Total temperature sensors. Rosemount Engineering Company Technical Bulletin 5755 (Rev. A), 29 pp. [Available from Rosemount Engineering Company, P.O. Box 35129, Minneapolis, MN 55435.]

Shaw, W. J., 1988: Inertial drift correction for aircraft-derived wind fields. *J. Atmos. Oceanic Technol.,* **5,** 774–782.

Tjernstrorm, M., and C. A. Friehe, 1991: Analysis of a radome airmotion system on a twin-jet aircraft for boundary-layer research. *J. Atmos. Oceanic Technol.,* **8,** 19–40.

Whitmore, S. A., T. R. Moes, and T. J. Larson, 1992: High angle-ofattack flush air data sensing system. *J. Aircraft,* **29,** 915–919.

Wyngaard, J. C., 1991: On the maintenance and measurement of scalar fluxes. *Land Surface Evaporation—Measurement and Parameterization,* T. J. Schmugge, and J.-C. Andre´, Eds., Springer- Verlag, 199–229.

-------, L. Rockwell, and C. A. Friehe, 1985: Errors in the measurement of turbulence upstream of an axisymmetric body. *J. Atmos. Oceanic Technol.,* **2,** 605–614.